Natural killer cells act as an extrinsic barrier for *in vivo* reprogramming

Elena Melendez[1], Dafni Chondronasiou[1], Lluc Mosteiro[2], Jaime Martínez de Villarreal[3], Marcos Fernández-Alfara[1], Cian Lynch[1], Dirk Grimm[4,5,6], Francisco X. Real[3], José Alcamí[7,8], Núria Climent[7], Federico Pietrocola[1,9], Manuel Serrano[1,10,*]

1 Institute for Research in Biomedicine (IRB Barcelona), Barcelona Institute of Science and Technology (BIST), Barcelona 08028, Spain
2 Department of Discovery Oncology, Genentech, South San Francisco, CA, 94080, USA
3 Epithelial Carcinogenesis Group, Spanish National Cancer Research Centre (CNIO), 28029, CIBERONC, Madrid, Spain
4 Dept. of Infectious Diseases/Virology, Medical Faculty, University of Heidelberg, 69120, Heidelberg, Germany
5 BioQuant, Cluster of Excellence CellNetworks, University of Heidelberg, 69120, Heidelberg, Germany
6 German Center for Infection Research (DZIF) and German Center for Cardiovascular Research (DZHK), partner site Heidelberg, 69120, Heidelberg, Germany
7 Hospital Clínic - Institut d'Investigacions Biomediques August Pi i Sunyer (IDIBAPS), 08036, Barcelona, Spain
8 AIDS Immunopathology Unit, National Center for Microbiology, Institute of Health Carlos III, 28220, Majadahonda (Madrid), Spain
9 Department of Biosciences and Nutrition, Karolinska Institutet, 14152 Huddinge, Sweden
10 Catalan Institution for Research and Advanced Studies (ICREA), Barcelona 08010, Spain

*Correspondence to: manuel.serrano@irbbarcelona.org

ABSTRACT

The ectopic expression of transcription factors Oct4, Sox2, Klf4 and Myc (OSKM) enables reprogramming of differentiated cells into pluripotent embryonic stem cells. Methods based on partial and reversible *in vivo* reprogramming are a promising strategy for tissue regeneration and rejuvenation. However, little is known about the barriers that impair reprogramming in an *in vivo* context. We report that natural killer (NK) cells significantly limit reprogramming, both *in vitro* and *in vivo*. Cells and tissues at the intermediate states of reprogramming upregulate the expression of NK activating ligands, such as MULT1 and ICAM1. NK cells recognize and kill partially reprogrammed cells in a degranulation-dependent manner. Importantly, *in vivo* partial reprogramming is strongly reduced by adoptive transfer of NK cells, whereas it is significantly improved by depletion of NK cells. Notably, in the absence of NK cells, the pancreatic organoids derived from OSKM-expressing mice are remarkably large, suggesting the generation of cells with progenitor properties. We conclude that NK cells pose an important barrier for *in vivo* reprogramming, and this concept may apply to other contexts of transient cellular plasticity.

Summary statement: Cellular reprogramming is inefficient *in vivo* and we report that this is due, in part, to the elimination of cells undergoing reprogramming by Natural Killer cells.

Keywords: reprogramming, pluripotency, plasticity, immune system, natural killer cells, NK receptor ligands, organoids

INTRODUCTION

The ectopic expression of the four transcription factors Oct4, Sox2, Klf4 and Myc (OSKM) enables reprogramming of differentiated cells into induced pluripotent stem cells (iPSCs) (Takahashi and Yamanaka, 2006). Reprogramming *in vivo*, within the context of an adult organism has been also achieved in mice with inducible transgenic expression of OSKM (Abad *et al.*, 2013; Ohnishi *et al.*, 2014). The process of reprogramming is typically inefficient, both *in vitro* and *in vivo*, and only a minority of cells reach full reprogramming. This is due, at least in part, to the existence of multiple cell-autonomous barriers, such as tumour suppressors, chromatin regulators, transcription factors, signalling pathways and micro RNAs (Haridhasapavalan *et al.*, 2020; Arabacı *et al.*, 2021). In contrast to the extensive knowledge on cell-intrinsic barriers, the extrinsic barriers that limit reprogramming remain largely unknown. In this

work, we have examined the composition of the immune cell infiltrate during *in vivo* reprogramming and we have identified a novel role of NK cells as a key barrier for reprogramming.

Transgenic OSKM expression *in vivo* triggers first the loss of cellular identity and formation of dysplastic areas across multiple tissues (Abad *et al.*, 2013; Ohnishi *et al.*, 2014). We refer to this intermediate state as “partial” reprogramming. Interestingly, at this stage, the effects of OSKM are reversible and tissues recover normal histology upon extinction of transgene expression (Ohnishi *et al.*, 2014). Continued expression of OSKM leads to cells expressing markers of embryonic pluripotency, which will ultimately form teratomas in various organs (Abad *et al.*, 2013; Ohnishi *et al.*, 2014). Currently, there is great interest in the potential of partial reprogramming as a strategy for rejuvenation and tissue repair. Ocampo *et al.* showed that short-term cyclic expression of OSKM improves physiological parameters after injury and extends lifespan in a model of premature aging, with negligible risk of teratoma formation (Ocampo *et al.*, 2016). In line with the pro-regeneration potential of *in vivo* partial reprogramming, transient OSKM (or OSK) expression has been demonstrated to enhance tissue repair in models of muscle injury (Chiche *et al.*, 2017; de Lázaro *et al.*, 2019), skin wound healing (Doeser, Schöler and Wu, 2018), optic nerve crush injury, glaucoma and aging-associated loss of vision (Lu *et al.*, 2020), and myocardial infarction (Chen *et al.*, 2021).

The capacity of the adaptive and innate immune cells to recognize and target pluripotent stem cells (PSCs) for elimination has been previously demonstrated. For instance, activated cytotoxic T lymphocytes (CTLs) have the ability to kill PSCs, including multipotent adult germ-line stem cells (maGSCs), embryonic stem cells (ESCs) and iPSCs in a peptide-dependent manner (Dressel *et al.*, 2009). Furthermore, natural killer (NK) cells (Frenzel *et al.*, 2009; Dressel *et al.*, 2010) and the complement system (Koch, Jordan and Platt, 2006) play a role in the rejection of stem cells *in vitro* and *in vivo* after implantation. NK cells also limit teratoma formation after subcutaneous injection of mouse ESCs, iPSCs and maGSCs (Dressel *et al.*, 2008) or human iPSCs (Benabdallah *et al.*, 2019). The sensitivity of PSCs to NK-mediated clearance has been ascribed to the downregulation of Major Histocompatibility Complex I (MHCI) on the surface of PSCs (a process known as ‘missing self’); and/or to the upregulation of NK-activating ligands (Dressel *et al.*, 2008, 2009, 2010; Frenzel *et al.*, 2009). In addition, IFNγ produced mainly by CTLs and NK cells hampers the final transition to pluripotency during *in vitro* reprogramming (Guo *et al.*, 2019). While the elimination of

pluripotent stem cells by the immune system is reasonably well understood, nothing is known about the intermediate state of partial reprogramming. It is currently unclear which immune subtypes infiltrate organs undergoing partial reprogramming, and to what extent they influence the outcome of *in vivo* reprogramming.

In the present study, we report that NK cells recognize and kill cells undergoing partial reprogramming. Furthermore, our results suggest that NK cells preferentially eliminate cells endowed with higher plasticity and regenerative capacity.

RESULTS

Partial reprogramming elicits immune infiltration in the pancreas

To interrogate whether the immune system plays a role in *in vivo* reprogramming, we first performed single-cell RNA sequencing (scRNAseq) analysis of the pancreas of mice with a doxycycline-inducible transgene expressing the four Yamanaka factors (*i4F*) and Wild Type (WT) mice, all treated with doxycycline for one week. Uniform Manifold Approximation and Projection (UMAP) representation showed an abundant infiltration of immune cells in response to reprogramming (**Fig. 1A**). Cell clusters were annotated according to their most significantly expressed markers (**Fig. 1B, S1**). We found that NK cells, T cells, neutrophils (NT), macrophages (Mϕ) and B cells were enriched in pancreata undergoing partial reprogramming (**Fig. 1B**) and their abundance was further supported by immunohistochemistry analysis (**Fig. S2**). Of note, the enrichment of NK cells was unique to the pancreas and was not observed in spleen and lymph nodes (**Fig. S3**). The relative abundance of other immune cell populations tested in spleen and lymph nodes remained unchanged, with the exception of macrophages and neutrophils, which were enriched in spleen (**Fig. S3**). We speculated that the magnitude of immune infiltration in the pancreas would positively correlate with the extent of tissue dysplasia evoked by OSKM expression. As previously reported, *i4F;p53*-null mice are more prone to undergo reprogramming than *i4F* mice with functional p53 (Mosteiro *et al.*, 2016). Accordingly, we found by flow cytometry a higher proportion of $CD45^+$ immune cells in *i4F;p53*-null pancreata compared to their *i4F* counterparts, indicating that the degree of reprogramming correlates with the extent of immune cell infiltration in the pancreas (**Fig. 1C)**. The most abundant cell types infiltrating the reprogramming pancreas belonged to the innate immune system, in particular, $F4/80^+$ and $CD11b^+$ cells (which mostly correspond to macrophages), $Gr1^+$ cells (which mostly correspond to neutrophils and myeloid derived suppressor cells or MDSCs), and NK cells (**Fig. 1C**). Of note, bulk transcriptomics analysis performed in

the pancreas of *i4F;p53*-null mice revealed a significant enrichment in NK cell cytotoxicity-associated genes (entry: mmu04650) compared to *i4F* mice (Mosteiro *et al.*, 2016) (**Fig 1D**). Based on these observations, we decided to study in detail the role of NK cells during reprogramming, and further below we also explore the role of macrophages and $Gr1^+$ cells.

NK cells eliminate partially reprogrammed cells *in vitro*

To investigate whether NK cells can directly interfere with the early stages of reprogramming, we performed co-culture experiments. Previous to this, we confirmed that our "co-culture medium" (containing IL-2 and IL-15) did not affect the function of NK cells or the reprogramming of fibroblasts, when tested separately (**Fig. S4A, S4B, S4C**). Then, we co-cultured primed splenic WT NK cells with *i4F* Mouse Embryonic Fibroblasts (MEFs) at different effector:target (E:T) ratios from day 2 to day 6 of *in vitro* reprogramming, which corresponds to the stage of partial reprogramming. At day 6, NK cells were removed from the culture and reprogramming was continued in standard iPSC medium until formation of iPSC colonies (scored at day 11) (**Fig. 2A**). Interestingly, we observed that the number of alkaline phosphatase (AP) positive iPSC colonies was inversely proportional to the number of NK cells in the medium (**Fig. 2B, 2C**). At the end of the reprogramming assay (day 11), those plates co-cultured with the highest amount of NK cells had no evidence of surviving fibroblasts, indicating a complete killing of the reprogramming fibroblasts (**Fig. 2C**). In contrast, non-reprogramming fibroblasts co-cultured with the same amount of NK cells remained viable at the end of the experiment (**Fig. 2C**). This result indicates that cells undergoing OSKM-induced reprogramming are targeted by NK cells for elimination.

NK receptors NKG2D (which binds to RAE1, MULT1 and H60 ligands in mouse cells) (Cerwenka *et al.*, 2000; Carayannopoulos *et al.*, 2002), LFA-1 (which interacts with ICAM1) (Chong *et al.*, 1994) and DNAM-1 (activated by CD155 in mouse) (Stanietsky *et al.*, 2013) have been described as major signalling molecules for NK activation. We studied the kinetics of expression of these ligands in reprogramming MEFs by flow cytometry. We observed upregulation of the NKG2D ligands H60 and MULT1 (**Fig. 2D**). In line with previous observations by flow cytometry (Schwarz *et al.*, 2018), we also detected a progressive upregulation of ICAM1 over the course of reprogramming. We did not observe upregulation of RAE1 and CD155. Taken together, these results show that cells undergoing reprogramming exhibit enhanced expression of a subset of NK stimulatory ligands. We next wondered whether NK-activating ligands

are also upregulated during *in vitro* human cell reprogramming. To address this question, we used previously published scRNAseq data from human dermal fibroblasts reprogrammed to naïve iPSCs (Liu *et al.*, 2020). Interestingly, these data show upregulation of the NK-activating ligand *MICB*, together with downregulation of NK-inhibitory ligands *HLA-A* and *HLA-E* (**Fig. S5**). These observations suggest that, similar to mouse cells, human cells undergoing reprogramming also become potential targets for NK cells.

To get mechanistic insights into the role of NK cells during *in vitro* reprogramming, we first asked whether NK cells require physical contact with partially reprogrammed target cells. To address this, we co-cultured primed NK cells with *i4F*-MEFs in transwell plates. We did not detect significant differences in the number of iPSC colonies between *i4F*-MEFs cultured with or without NK cells in transwells (**Fig. 2D**). We then tested, in direct co-culture conditions, the involvement of cytotoxic granules in the killing process by using the v-ATPase inhibitor Concanamycin A (ConA), which prevents the release of lytic granules by activated NK cells. The presence of ConA abolished the inhibitory action of NK cells on iPSC formation (**Fig. 2E**). Collectively, these data indicate that partially reprogrammed cells are lysed by NK cells in a process involving direct contact with their target and release of lytic granules.

To evaluate the implication of the NKG2D/ligand interaction in NK cell-mediated recognition and elimination of cells undergoing reprogramming, we co-cultured NK cells and *i4F*-MEFs with an NKG2D blocking antibody or with the corresponding isotype control. Under this setting, we found that anti-NKG2D treatment partially suppressed the inhibitory effect of NK cells on reprogramming (**Fig. 2F**). Therefore, these data demonstrate that NK cells target early reprogramming cells, at least in part, via engagement of the NKG2D receptor.

NK cells activate and degranulate during *in vivo* reprogramming

To dissect the role of NK cells recruited to the pancreas during *in vivo* reprogramming, we analysed the expression of NK-activating ligands in the pancreata of *i4F* mice at an intermediate stage of reprogramming (7 days of doxycycline treatment). In line with our *in vitro* observations, NK-activating ligands were transcriptionally upregulated in the pancreata of *i4F* mice compared to their WT counterparts. By flow cytometry of non-immune cells ($CD45^-$ cells), we observed significant upregulation of RAE1, MULT1, ICAM1 and CD155 ligands in pancreas undergoing partial (**Fig. 3A**). This was accompanied in some cases by an increase in mRNA levels, as it was the case of

Icam1 and *Cd155* (**Fig. 3B**). We surmise that the different behaviour of CD155 in pancreas *versus* cultured fibroblasts reflects cell type specific differences. These results prompted us to examine the localization of infiltrating NK cells in the pancreata of partially reprogrammed mice. Notably, we found NK cells directly surrounding dysplastic cells in pancreas undergoing partial reprogramming (**Fig. 3C**). In control pancreas, NK cells were only detected within the blood vessels. To further characterize the NK cells infiltrating pancreas during the process of reprogramming, we used cell surface markers to profile the activation status of NK cells at different time points (**Fig. 3D**). We observed a modest transient cell surface increase of NKG2D at day 3. The transient nature of NKG2D elevation in the cell surface is consistent with the idea that NKG2D engagement by membrane-bound ligands triggers its internalization, which is necessary for intracellular signalling (Coudert *et al.*, 2005; Oppenheim *et al.*, 2005; Wiemann *et al.*, 2005). Interestingly, as early as 5 days after initiating reprogramming, NK cells significantly upregulated the degranulation marker CD107a (also known as LAMP-1) (Alter, Malenfant and Altfeld, 2004). Finally, we also observed an upregulation of the inhibitory receptors Ly49CI and NKG2A, likely reflecting a progressive exhaustion (Ablamunits *et al.*, 2011; Sun *et al.*, 2017). Interestingly, double positive $CD107a^{+}$ $NKG2A^{+}$ NK cells were progressively upregulated as reprogramming progressed, and these markers separately were highly positively correlated, suggesting an association between degranulation and inhibition of NK cells. Collectively, these findings indicate that, upon infiltrating the reprogramming pancreas, NK cells manifest hallmarks of activation, including degranulation and upregulation of inhibitory receptors.

NK cells are a barrier for *in vivo* reprogramming in the pancreas

Based on the above findings, we hypothesized that NK cells might limit *in vivo* reprogramming. We first addressed the question of whether the activity of NK cells is affected by the activation of our transgenic OSKM allele. We confirmed that the OSKM transgene is upregulated in splenic NK cells after 7 days of treatment of *i4F* mice with doxycycline (**Fig. S6A**). We then isolated NK cells from the spleen of *i4F* and WT mice treated with doxycycline for 5 days *in vivo*. These NK cell isolates were then primed *in vitro* during 6 days with cytokines IL-2 and IL-15, while maintaining the presence of doxycycline. Finally, NK activity was measured using YAC-1 as target cells, which are sensitive to NK clearance due to the lack of MHCI expression (Cikes, Friberg Jr. and Klein, 1973). The percentage of dead ($DAPI^{+}$) YAC-1 cells did not vary between WT and *i4F* NK cells (**Fig. S6B**). This result indicates that the expression of our

reprogramming OSKM cassette does not significantly alter the activity of NK cells during the time frame of *in vivo* reprogramming studied in the pancreas.

Having established that NK activity is not significantly affected by OSKM expression in our mouse model, we then addressed the effect of eliminating NK cells on partial reprogramming. For this, we depleted NK cells using a monoclonal antibody against NK1.1 and NK depletion was confirmed by flow cytometry using anti-NKp46 (**Fig. 4A, 4B**). We noted that NK1.1-depleted reprogrammed mice suffered a more profound weight loss than reprogrammed mice treated with isotype control (**Fig. S7A**). Moreover, serum amylase levels, which increase proportionally to the levels of dysplasia in our mouse model (**Fig. S7B**), were significantly upregulated in anti-NK1.1-treated *i4F* mice compared to isotype control-treated *i4F* mice (**Fig. S7C**). Histologically, the absence of NK1.1$^+$ cells resulted in larger areas of pancreatic dysplasia and a higher number of NANOG$^+$ cells, a marker of the late stages of reprogramming (**Fig. 4C**). Based on these results, we propose that NK cells hinder the process of *in vivo* reprogramming by eliminating emerging partially reprogrammed cells. To further strengthen this hypothesis, we tested whether the adoptive transfer of exogenous NK cells could reduce the normal levels of reprogramming in the pancreas. Thus, NK cells from WT donor mice were injected at day 3 of reprogramming. Importantly, exogenous transfer of NK cells dramatically reduced the efficiency of reprogramming, and no NANOG$^+$ cells were detected (**Fig. 4C**).

We wondered whether NK cells could have a role in other models of tissue plasticity in the pancreas. In particular, we focused on caerulein-treatment, which is known to induce acinar-to-ductal metaplasia (ADM), a histological lesion that also implies reversible changes in cell identity (Shibata *et al.*, 2018). Importantly, NK1.1$^+$ cell ablation did not alter the amount of caerulein-induced ADM (**Fig. 4D**). These results reinforce the concept that NK cells are particularly relevant during *in vivo* partial reprogramming.

Finally, we focused on two other immunological cell populations that also infiltrate the pancreas during reprogramming, namely, macrophages and Gr1$^+$ cells, the latter including neutrophils and MDSCs (**Fig. 1C**). Clodronate-mediated depletion of phagocytic cells (**Fig. 5A, 5B**) failed to significantly modify the reprogramming process (**Fig. 5C**). To deplete Gr1$^+$ cells, we used an anti-Gr1 antibody (clone RB6-8C5) that recognizes the antigenic markers Ly6G and Ly6C, mostly expressed in neutrophils and MDSCs (**Fig. 5D, 5E**). Interestingly, anti-Gr1 treatment strongly reduced

reprogramming in the pancreas (**Fig. 5D**). Considering that neutrophils and MDSCs suppress the activity of NK cells in different contexts, such as cancer (Bruno *et al.*, 2019; Li *et al.*, 2020; Sun *et al.*, 2020; Zalfa and Paust, 2021), these results are consistent with a scenario where NK cells eliminate cells undergoing reprogramming and, at the same time, NK cells are negatively regulated by infiltrating $Gr1^+$ cells.

NK cells are a barrier for *in vivo* reprogramming in the liver

To further test the role of NK cells during *in vivo* reprogramming, we shifted to a different experimental model previously reported by us, based on the delivery of the four Yamanaka factors using adeno-associated viruses (AAV) (Senís *et al.*, 2018). In particular, WT mice were inoculated with a mixture of AAV8 viruses, which exhibit high tropism for the liver (Zincarelli *et al.*, 2008), carrying each of the four Yamanaka factors and GFP. As a readout, rather than testing partial reprogramming, we chose for simplicity to allow the process to continue until full reprogramming and the subsequent formation of teratomas (**Fig. 6A**). Importantly, further supporting the negative role of NK cells during *in vivo* reprogramming NK1.1-depleted mice developed teratomas earlier than mice with NK cells (**Fig. 6B**). These observations are compatible with the idea that NK cells act as a general barrier for reprogramming in the liver, similar to what we have reported in the pancreas. In this case, however, we cannot discriminate whether NK cells are acting at the partial reprogramming stage and/or at the later stages of reprogramming and teratoma formation.

Depletion of $NK1.1^+$ cells allows the survival of highly plastic pancreatic cells

To further investigate the role of NK cells as a barrier for reprogramming, we used an *ex vivo* system based on pancreatic organoids as a proxy to monitor the abundance of cells with stem cell-like properties (Clevers, 2016). We reprogrammed mice for 7 days, while treating them with isotype control or anti-$NK1.1^+$ antibodies (**Fig. 7A**). We then prepared single cell pancreatic extracts, and an equal number of cells per condition were embedded in Matrigel. All organoids grew as homogeneous, hollow spheres composed of a single-layer epithelium, as previously described (Huch *et al.*, 2013). Interestingly, at day 5 post-embedding, organoids originating from anti-NK1.1-treated animals were significantly larger than the ones derived from *i4F* mice treated with isotype control (**Fig. 7B**) and, at day 8, the size difference was evident even macroscopically (**Fig. 7B**). This observation demonstrates that NK cells eliminate partially reprogrammed cells endowed with high plasticity and capacity to form organoids.

DISCUSSION

In this study, we provide direct evidence that the host immune system and, specifically NK cells, targets partially reprogrammed cells during the first stages of OSKM expression. We show that NK depletion using antibodies significantly improves the efficiency of *in vivo* reprogramming, both in the pancreas and in the liver. Conversely, when exogenous NK cells are adoptively transferred to an *i4F* mouse host, dysplastic areas in the pancreas, indicative of partial reprogramming, are barely detectable. These data, together with the infiltration of NK cells in the dysplastic tissue, support the notion that NK cells eliminate cells undergoing reprogramming.

Our data also provide insights into the mechanisms by which NK cells target reprogrammed cells. We show *in vivo* and *in vitro* that partially reprogrammed cells upregulate NK-activating ligands. In particular, we observe *in vivo* the upregulation of MULT1, ICAM1 and CD155, which bind and activate, respectively, the NK receptors NKG2D, LFA1, and DNAM1. All these receptors are known to stimulate NK killing activity towards target cells expressing their cognate ligands (Chong *et al.*, 1994; Cerwenka *et al.*, 2000; Carayannopoulos *et al.*, 2002; Stanietsky *et al.*, 2013). The NKG2D receptor is one of the best known stimulating receptors and is relevant in multiple processes involving NK cells, including autoimmune diseases, viral and bacterial infections, and rejection of transplants (Siemaszko, Marzec-przyszlak and Bogunia-kubik, 2021). In our *in vitro* co-culture system, blocking anti-NKG2D antibodies partially rescued the formation of iPSCs colonies despite the presence of NK cells. We conclude that NKG2D binding is an important process for the activation of NK cells during partial reprogramming. Our results do not exclude the potential contribution of other stimulating receptors, such as LFA1 and DNAM1, to the negative effect of NK cells on reprogramming.

During *in vivo* reprogramming, the protein levels of NKG2D detected by cytometry modestly increased at the early reprogramming phase although did not reach statistical significance and rapidly returned to normal levels. This is in line with the concept that NKG2D engagement leads to its endocytosis and this is important for the appropriate activation of NK cells (Coudert *et al.*, 2005; Oppenheim *et al.*, 2005; Wiemann *et al.*, 2005). We also observed an increase in the cell surface expression of the NK-inhibitory receptor NKG2A. This inhibitory receptor has been associated to NK cell exhaustion in humans (Ablamunits *et al.*, 2011; Sun *et al.*, 2017). Parallel to NKG2A, we also observed a progressive upregulation of the degranulation marker CD107a. Collectively, these findings indicate that NK cells infiltrate partially

reprogrammed pancreata and, upon exposure to NK-activating ligands, release lytic granules, and upregulate inhibitory receptors possibly as part of the acquisition of an exhausted phenotype.

Our cytometry data indicated that multiple immune populations, notably macrophages, MDSCs and neutrophils accumulate in the pancreas upon *in vivo* reprogramming. We did not detect significant changes in reprogramming efficiency when macrophages were depleted using clodronate liposomes. We surmise that this may reflect the presence of macrophage subpopulations with opposing effects on reprogramming, which is in line with the high heterogeneity and plasticity of macrophages. In contrast to macrophages, depletion of MDSCs and neutrophils significantly reduced *in vivo* reprogramming in the pancreas. It has been extensively described that MDSCs suppress NK functions in different contexts, such as hepatitis C virus (HCV) infection (Celeste C. *et al.*, 2016), hepatocellular carcinoma (HCC) (Hoechst *et al.*, 2009) and other types of solid and haematological malignancies (Tumino *et al.*, 2021; Zalfa and Paust, 2021). Similarly, intra-tumoral MDSCs induce suppression of $CD8^+$ T cells (Baumann *et al.*, 2020). Neutrophils also impair the cytotoxicity and infiltration capability of NK cells in cancer (Spiegel *et al.*, 2016; Li *et al.*, 2020; Sun *et al.*, 2020). Therefore, our data are compatible with a model in which $Gr1^+$ cells counteract the cytotoxic activities of NK cells against partially reprogrammed cells.

We wondered whether depletion of NK cells during OSKM expression could facilitate the emergence of cells with progenitor features. To explore this, we examined the capacity of partially reprogrammed pancreatic cells to form organoids. Interestingly, pancreatic organoids derived from NK-depleted mice grew significantly more compared to organoids derived from mice treated with an isotype control. This suggests that the absence of NK cells facilitates the formation of progenitor-like cells *in vivo* upon OSKM expression. In the future, it will be relevant to explore whether organoids from NK-depleted partially-reprogrammed tissues display better engraftment properties, and improve tissue regeneration after tissue injury.

Cellular dedifferentiation is emerging as a general process during tissue repair and regeneration (Yao and Wang, 2020). The insights obtained in our study, which also involve *in vivo* dedifferentiation, could be applicable to pathophysiological settings of tissue repair that involve inflammatory cells and, in particular, NK cells.

MATERIAL AND METHODS

Mice

All mice were bred and maintained at the animal facilities of the Barcelona Science Park in strict accordance with the Spanish and European Union regulation. Animal procedures were performed according to protocols approved by the Animal Care and Use Ethical Committee (IACUC) of Barcelona Science Park and the Catalan Government. Mice were housed at specific pathogen free (SPF) barrier area with access to *ad libitum* standard chow diet. Animal experiments were designed and conducted with consideration of the ARRIVE guidelines and mice were sacrificed when they presented signs of morbidity in accordance to the *Guidelines for Humane Endpoint for Animals Used in Biomedical Research* from the Council for International Organization of Medical Sciences (CIOMS). Reprogrammable *i4F* mouse was previously generated in the laboratory in a pure C57BL/6J.Ola.Hsd genetic background (Abad *et al.*, 2013). *i4F-B* strain contains an ubiquitous doxycycline-inducible transgene encoding for the four Yamanaka factors *Oct4, Sox2, Klf4* and *cMyc* (OSKM) inserted in the *Pparg* gene and the rtTA within the *Rosa26* locus. All mice were heterozygous for both OSKM and rtTA transgenes. All experiments were performed with male and female mice of 8-16 weeks of age.

Animal procedures

Doxycycline hyclate BioChemica (PanReac, A2951, Spain) was administered in the drinking water (1 mg/ml) supplemented with 7.5% sucrose for 7 days. Immune populations were depleted by intraperitoneal injection of 200 µg of anti-NK1.1 (clone PK136, BioxCell, New Hampshire, USA) or 200 µg of anti-Gr1 (clone RB6-8C5, BioxCell) at days -1, 3 and 5 of reprogramming. Isotypes control IgG2a (clone C1.18.4, BioxCell) and IgG2b (clone LTF-2, BioxCell) were used in control groups, respectively. For the depletion of macrophages, mice received 200 µl of either clodronate or empty liposomes (Clodronate Liposomes, The Netherlands) retro-orbitally at days 1, 3 and 6 of reprogramming. Mild acute pancreatitis was induced by 7 intraperitoneal injections, given once per hour, of a pancreatic secretagogue cholecystokinin (CCK) analogue called caerulein (Bachem, Switzerland) at 100 µg/kg for 2 consecutive days. A second group of control animals received injections of PBS only. Mice were sacrificed at day 4 after the first injection. All animals were sacrificed by cervical dislocation, unless blood extraction from the heart was performed. In that case, mice were sacrificed in a CO_2 chamber.

NK cell isolation and adoptive transfer

NK cells were enriched from the spleen of WT C57BL/6J mice via negative selection (Miltenyi Biotec NK cell isolation kit, 130-115-818, Germany) and treated with 50 U/ml IL-2 (PeproTech, 212-12, UK) and 50 ng/ml IL-15 (PeproTech, 210-15) for 24h in 96 well-plate with U-bottom shape (1 x 10^5 NK cells/well). NK cell culture medium was composed by RPMI-1640 (Sigma, R8758, St. Louis, USA) supplemented with 10% FBS, 2 mM L-glutamine, 100 µg/ml penicillin-streptomycin, 10 mM HEPES, non-essential amino acids (all from Life Technologies, Massachusetts, USA), and 0.5 mM sodium pyruvate (Gibco, Massachusetts, USA). Next day, 3.8 x 10^6 NK cells were injected retro-orbitally into recipient mice in 150 µl of PBS at day 3 of reprogramming.

scAAV8 injections

AAV8 virus were kindly provided by Dr. Dirk Grimm (Heidelberg University Hospital, Germany) and were produced as described elsewhere (Senís *et al.*, 2018). WT male mice were retro-orbitally injected with scAAV8 SFFV-hCO-O/K/S/M vectors at doses of 1 x 10^{11} vg/vector. A scAAV8 vector encoding GFP was added as tracer at the same concentrations. During the whole experiment, 200 µg of anti-NK1.1 (clone PK136, BioxCell) or its isotype control, IgG2a (clone C1.18.4, BioxCell), were injected intraperitoneally at days -1, 3 and 5 during the first week, and then once a week until the end of the experiment. Mice were sacrificed when teratomas were palpable.

Single cell preprocessing and analysis

To isolate all pancreatic cell types, tissue was digested using 1 mg/ml Collagenase P (Sigma, 11213865001), 2 U/ml Dispase II (Life Technologies, 17105041), 0.1 mg/ml Soybean Trypsin Inhibitor (Life Technologies, 17075-029) and 0.1 mg/ml DNase I (Sigma, D4513) in HBSS with Ca^{2+}/Mg^{2+} (Life Technologies, 14025050). Tissue dissociation was performed using the gentle MACS™ Octo Dissociator (Miltenyi Biotech) at 37°C for 40 min. The tissue was further digested with 0.05% Trypsin-EDTA (Life Technologies, 25300062) for 5 min at 37°C and erythrocytes were removed with red blood cell lysis buffer (Biolegend, 420301, San Diego, US). Cells were loaded onto a 10x Chromium Single Cell Controller chip B (10x Genomics) as described in the manufacturer's protocol (Chromium Single Cell 3' GEM, Library & Gel Bead Kit v3, PN-1000075). Generation of gel beads in emulsion (GEMs), barcoding, GEM-RT clean up, cDNA amplification, and library construction were performed following the manufacturer's recommendations. Libraries were loaded at a concentration of 1.8 pM and sequenced in an asymmetrical pair-end format in a NextSeq500 instrument (Illumina, San Diego, US). For data analysis, chromium 10X v3 sequencing files were

demultiplexed, aligned to reference genome (GRCm38/mm10) and count were generated using Cell Ranger software. Barcodes, features and count matrices were loaded into Seurat (v3) for downstream analysis. Each condition (WT and *i4F*) was analysed separately as a merge from the corresponding replicates. Ambient RNA contamination was estimated and corrected using SoupX (Young and Behjati, 2020). Cells expressing < 150 genes and > 5% of mitochondrial genes were excluded. Dimensionality of the datasets was set to the first 20 principal components based on the result of the JackStraw analysis and the stabilization of the elbow plot. Normalization was carried out using SCTranform function (Hafemeister and Satija, 2019). Cluster stability was visualized at different resolutions using clustree (Zappia and Oshlack, 2018). Resolution was set to 0.2 for the two datasets (WT and *i4F*). Clusters were manually annotated based on the significant markers using FindAllMarkers function. Immune cells for each dataset were extracted as raw counts and merged together for the immune combined analysis. Normalization, dimensionality reduction, clustering and cell annotation was carried out in the immune dataset as mentioned before. All the datasets were visualized using UMAP projection (Becht *et al.*, 2019).

Amylase analysis

Serum was obtained from WT (*n*=6) and *i4F* mice treated with isotype control (*n*=6) or anti-NK1.1 antibodies (*n*=6) at day 7 of doxycycline (1 mg/ml) administration in water. Samples were analysed with an amylase kit (Spinreact, SP41201, Spain) in a Spinlab 100 (Spinreact, 9-9059) machine.

Cell culture

Primary Mouse Embryonic Fibroblasts (MEFs) were obtained from *i4F* embryos at E13.5 as previously described (Serrano *et al.*, 1997). MEFs were maintained in Dulbecco's modified Eagle's medium (DMEM) (Gibco) supplemented with 10% heat inactivated Fetal Bovine Serum (FBS) (Gibco) and penicillin-streptomycin (Gibco). At passage 1, 6 x 10^4 MEFs were seeded in 12 well-plates (Corning, Corning, USA) or 3 x 10^6 MEFs were seeded in 6 well-plates (Corning), according to the experiment, and cultured with "iPSC medium", composed by high glucose DMEM (Gibco) supplemented with 15% of KnockOut Serum Replacement (KSR) (Life Technologies), LIF (1000 U/ml) (Merck Chemicals, Germany), non-essential amino acids, penicillin-streptomycin (Gibco) and 100 μM β-mercaptoethanol (Life Technologies, 31350010). Cells were treated with doxycycline (Sigma) at 1 μg/ml to induce OSKM-cassette expression. Medium was changed every other day until iPSC colonies appeared at day 11. Cells

were then fixed with 4% paraformaldehyde (Aname S.L, Spain), washed with PBS and incubated from 30 minutes to 1 hour in Alkaline Phosphatase (AP) staining solution (AP Blue Membrane Substrate Solution, Sigma). AP^+ colonies per well were scored to determine the efficiency of reprogramming. Cells were maintained in a humidified incubator at 37 °C with 5% CO_2. Cultures were routinely tested for mycoplasma and were always negative.

Co-culture experiments

For co-culture experiments, NK cells were isolated and activated *in vitro* overnight as described above. NK cells were co-cultured with MEFs from day 2 to day 6 of *in vitro* reprogramming in "co-culture medium", containing DMEM (containing L-glutamine and sodium Pyruvate) (Life Technologies) supplemented with 10% FBS (Life Technologies), LIF (1000 U/ml) (Merck Chemicals), non-essential amino acids (Life Technologies), 10 mM HEPES, penicillin-streptomycin (Gibco), 100 µM β-mercaptoethanol (Life Technologies), 50 U/ml IL-2 (PeproTech, 212-12), 50 ng/ml IL-15 (PeproTech, 210-15) and doxycycline (1 µg/ml, Sigma). At day 6, NKs were removed and the culture was washed with PBS once before adding "iPSC medium" with doxycycline. *In vitro* reprogramming continued until the appearance of iPSC colonies around day 11. E:T ratios were 0.5:1, 2.3:1 and 4.5:1. Reprogrammed MEFs non-co-cultured with NK cells were also cultured in the presence of "co-culture medium" from day 2 to day 6. To test the mechanism of killing, NK:MEF co-culture was performed in the presence of the granule exocytosis inhibitor Concanamycin A (100 nM, Merck Life Science S.L.U, 27689) at E:T ratio of 1:1. For the transwell experiment, NK cells were seeded on top of 12 mm Transwell® with 0.4 µm Pore Polycarbonate Membrane Insert (Corning, 3401) at day 2 of reprogramming (E:T ratio 1:1). Transwells were removed at day 6 of reprogramming. NKG2D receptor was blocked by adding mouse NKG2D/CD314 antibody (20 µg/ml) (Bio-Techne R&D Systems S.L, MAB1547-500, Minnesota, USA) to the co-culture at days 2 and 4 of reprogramming (E:T ratio 1:1). All co-culture experiments were performed in 12 well-plates (Corning). For cytotoxic assays, YAC-1 cells were kindly donated by Dr. Domingo Barber (CNB-CSIC). NK cells were isolated from *i4F* and WT mice treated with doxycycline for 5 days. They were primed *in vitro* with IL-2 and IL-15 in the presence of doxycycline (1 µg/ml) for 6 days, and they were co-cultured with YAC-1 cells for 4h. $DAPI^+$ YAC-1 cells were quantified by flow cytometry.

Pancreatic organoids

Pancreas were dissociated to the single cell level as described above. For all experimental conditions, the same number of cells (3 x 10^5) were embedded in 200 µl growth factor reduced Matrigel drops (Corning, 356231) and cultured in pancreatic organoid medium, as described previously (Huch *et al.*, 2013). Medium was refreshed every 2-3 days and it was supplemented with doxycycline (1 µg/ml) to activate the OSKM cassette. At day 5 after seeding, 10 representative 4x fields per sample were taken to measure organoid size using Image J software. All analysis were conducted in a blinded way.

Reverse transcription-PCR (RT-PCR)

For *in vitro* experiments, total RNA was extracted from MEFs with Trizol (Invitrogen, Massachusetts, USA), following the providers recommendations. 1 µg of total RNA was retrotranscribed into cDNA using iScript cDNA Synthesis kit (BioRad, 170-8891, California, USA). For pancreas samples, total RNA was isolated by acid guanidinium thiocyanate-phenol-chloroform extraction. Up to 5 µg of total RNA was reverse transcribed into cDNA using iScriptTM Advanced cDNA Synthesis Kit (BioRad, 172-5038). Quantitative real time-PCR was performed suing Sybr Green Power PCR Master Mix (Promega Biotech, A6002, Wisconsin, USA) in a QuantStudio 6 Flex thermocycler (Applied Biosystem, Massachusetts, USA). *Gapdh* served as endogenous normalization control. Primers used are listed in **Table S1**.

Immunohistochemistry of tissue samples

Samples were fixed overnight at 4ºC with neutral buffered formalin (HT501128-4L, Sigma-Aldrich). Paraffin-embedded tissue sections (2-3 µm) were dried at 60ºC over-night and dewaxed. For Haematoxylin eosin staining, a standard protocol using CoverStainer (Dako-Agilent, California, USA) was performed. For some antibodies, immunohistochemistry was performed using a Ventana discovery XT for 60 min: Nanog D2A3 (Cell Signaling, 8822, Massachusetts, USA) at 1:100 - 1:250, F4/80 (eBioscience, clone BM, 14-4801-85) at 1:100 and B220 (BD Biosciences, 550286, New Jersey, USA) at 1:200. For the rest of antibodies, immunohistochemistry was performed manually or with the Leica Bond RX platform: CD3 (Dako-Agilent, 11503) at 1:10 for 120 min, CD4 (Sino Biological, 50134R001) at 1:2000 for 120 min, CD8α [EPR20305] (Abcam, ab209775, UK) at 1:1000 for 120 min, Klrb1c/CD161c (E6Y9G) (encoding NK1.1 antigen) (Cell Signaling, 39197S) at 1:500 for 120 min, NE (Abcam, ab68672) at 1:1000 for 120 min and FoxP3 (Cell Signaling, 12653) at 1:750 for 60 min. Antigen retrieval for Nanog and B220 was performed with Cell Conditioning 1 (CC1)

buffer (Roche, 950-124, Switzerland) and for F4/80 with proteinase K (Dako-Agilent, S3020) for 5 min at room temperature (RT). Secondary antibodies used were the OmniMap anti-Rat HRP (Roche, 760-4457) or OmniMap™ anti-Rb HRP (Roche, 760-4311). Blocking was done with Casein (Roche, 760-219). Antigen-antibody complexes were revealed with ChromoMap DAB Kit (Roche, 760-159). For CD3, CD4, CD8α, NE, FoxP3 and Klrb1c/CD161c, antigen retrieval was performed with BOND Epitope Retrieval Solution 2 (Leica Biosystems, AR9640, Germany) or with Envision FLEX Target retrieval Solution HIGH pH (Dako-Agilent, K8004) or with Trizma Base/EDTA pH 9.0 (T6066-1 Kg, E51345006). Blocking was performed with Peroxidase-Blocking Solution at RT (Dako-Agilent, S2023) and 5 % of goat normal serum (Life Technology, 16210064) mixed with 2.5 % BSA diluted in wash buffer for 10 and 60 min at RT. The secondary antibody used was the BrightVision poly HRP-Anti-Rabbit IgG, incubated for 45 min (ImmunoLogic, DPVR-110HRP, California, USA) or the polyclonal Goat Anti-Mouse (Dako-Agilent, P0447). Antigen–antibody complexes were revealed with 3-3′-diaminobenzidine (Leica Biosystems, RE7230-K). Sections were counterstained with hematoxylin (Dako-Agilent, CS700) and mounted with Mounting Medium, Toluene-Free (Dako-Agilent, CS705) using a Dako CoverStainer. Specificity of staining was confirmed by staining with a rat IgG (R&D Systems, 6-001-F, Minneapolis, USA), mouse IgG (Abcam, ab37355) or a Rabbit IgG (Abcam, ab27478) isotype controls. Brightfield images were acquired with a NanoZoomer-2.0 HT C9600 digital scanner (Hamamatsu, Japan) equipped with a 20x objective.

Image analysis

Brightfield images of immunohistochemistry were quantified in a blinded way using QuPath software 0.1.2 (Bankhead *et al.*, 2017) with standard DAB detection methods. Reprogramming efficiency was evaluated and quantified by histopathological assessment of dysplastic areas in the pancreas.

Flow cytometry

Blood to assess immune cells depletion was collected in Microvette® EDTA-coated tubes (16.444, Laborimpex, Belgium) and incubated with red blood cell lysis buffer (Biolegend, 420301) for 5 min. Cells were then washed once with PBS and pre-incubated for 5 min with Mouse BD Fc Block™ containing purified anti-mouse CD16/CD32 mAb 2.4G2 at 1 µg/1 million cells in 100 µl (BD Biosciences, 553142) of FACS buffer (0.5% BSA and 5 mM EDTA in PBS) for 15 min at 4°C. After a washing step with FACS buffer, cells were incubated with the appropriate antibody for 40 min at 4°C (**Table S2**). For the analysis of infiltrating immune cell populations, pancreas were

digested as previously described and immune cell types were stained following the same protocol (**Table S2**), but keeping the samples at RT. Spleen and inguinal lymph nodes were mechanically processed into single cell suspension. Erythrocytes were lysed using isotonic ammonium chloride solution before performing antibody staining. Single cell suspensions were subsequently incubated with TruStain FcX™ (anti-mouse CD16/32) antibody (1:100, Biolegend, 101320) for 10 minutes on ice. After a washing step with FACS buffer, cells were incubated with the appropriate antibody for 20 min at 4°C (**Table S2**). After 3 washes with FACS buffer, DAPI Fixable Violet was used to exclude dead cells. FACS analyses were performed using a Gallios Flow Cytometry System (Beckman Coulter) or a FACSAria Fusion (BD Biosciences) with with BD FACSDiva software (v.8.0.1), depending on the experiment.

For the characterization of NK cell surface receptors, pancreatic cells were stained with the LIVE/DEAD™ Fixable Blue Dead Cell Stain Kit (Thermo Fisher Scientific, L23105, Massachusetts, US) for 15 min to evaluate viability. After a washing step with PBS, cells were incubated for 20 min with a combination of anti-mouse antibodies (**Table S2**). Isotype control antibodies were used as negative controls. Cells were analysed with a BD LSRFortessa™ Flow Cytometer. All data were analysed by FlowJo v10 software (BD Biosciences) and GraphPad Prism 9.0.1.

Statistical analysis

The data were analysed using GraphPad Prism v.9.0.1 software and represented as mean ± SD or mean ± SEM of independent biological replicates (mice or clones of MEFs). Statistical analyses were performed using an unpaired two-tailed Student's t-test to compare the means between two different groups. Means of multiple groups were compared by one-way analysis of variance (ANOVA). Differences were considered significant based on the P value (*P<0.05;**P < 0.01; ***P < 0.001; ****P < 0.0001).

Acknowledgements

We thank Domingo Barber (CNB-CSIC, Madrid) for kindly providing us YAC-1 cells. We are grateful to Maria Isabel Muñoz for her assistance with the animal protocols. We acknowledge the IRB core Facilities for their support and the Barcelona Science Park Animal Facility for animal maintenance.

Competing interests

M.S. is shareholder of Senolytic Therapeutics, S.L., Rejuveron Senescence Therapeutics, A.G., and Life Biosciences, Inc.

Author contributions

E.M. designed and performed most experiments, contributed to data analysis, discussion and writing the manuscript. E.M., D.C., L.M., N.C., M.F, C.L and F.P. provided general experimental support. J.M. and F.X.R. analysed the scRNA-seq data. J.A. provided technical guidance on NK cell cytometry analysis. D.G. provided reagents. M.S. designed and supervised the study, secured funding, analysed data and co-wrote the manuscript. All authors discussed the results and commented on the manuscript.

Funding

E.M was funded by an IRB Future Fellowship from the Institute for Research in Biomedicine. Work in the laboratory of F.X.R. was funded by a grant from the Spanish Ministry of Science co-funded by the European Regional Development Fund (ERDF) (RTI2018-101071-B-I00). Work in the laboratory of J.A. at Hospital Clínic was funded by “la Caixa” Foundation. Work in the laboratory of M.S. was funded by the IRB and “la Caixa” Foundation, and by grants from the Spanish Ministry of Science co-funded by the European Regional Development Fund (ERDF) (SAF2017-82613-R), European Research Council (ERC-2014-AdG/669622), and Secretaria d'Universitats i Recerca del Departament d'Empresa i Coneixement of Catalonia (Grup de Recerca consolidat 2017 SGR 282).

Data availability

Generated scRNA-seq datasets have been deposited in GEO under accession number GSE188819.

REFERENCES

Abad, M. *et al.* (2013) ‘Reprogramming in vivo produces teratomas and iPS cells with totipotency features’, *Nature*, 502(7471), pp. 340–345. doi: 10.1038/nature12586.

Ablamunits, V. *et al.* (2011) ‘NKG2A is a marker for acquisition of regulatory function by human CD8+ T cells activated with anti-CD3 antibody’, *European Journal of Immunology*, 41(7), pp. 1832–1842. doi: 10.1002/eji.201041258.

Alter, G., Malenfant, J. M. and Altfeld, M. (2004) 'CD107a as a functional marker for the identification of natural killer cell activity', *Journal of Immunological Methods*, 294(1–2), pp. 15–22. doi: 10.1016/j.jim.2004.08.008.

Arabacı, D. H. *et al.* (2021) 'Going up the hill: chromatin-based barriers to epigenetic reprogramming', *FEBS Journal*, 288(16), pp. 4798–4811. doi: 10.1111/febs.15628.

Bankhead, P. *et al.* (2017) 'QuPath: Open source software for digital pathology image analysis', *Scientific Reports*, 7(1), pp. 1–7. doi: 10.1038/s41598-017-17204-5.

Baumann, T. *et al.* (2020) 'Regulatory myeloid cells paralyze T cells through cell–cell transfer of the metabolite methylglyoxal', *Nature Immunology*, 21(5), pp. 555–566. doi: 10.1038/s41590-020-0666-9.

Becht, E. *et al.* (2019) 'Dimensionality reduction for visualizing single-cell data using UMAP', *Nature Biotechnology*, 37(1), pp. 38–47. doi: 10.1038/nbt.4314.

Benabdallah, B. *et al.* (2019) 'Natural Killer Cells Prevent the Formation of Teratomas Derived From Human Induced Pluripotent Stem Cells', *Frontiers in Immunology*, 10, pp. 1–9. doi: 10.3389/fimmu.2019.02580.

Bruno, A. *et al.* (2019) 'Myeloid Derived Suppressor Cells Interactions With Natural Killer Cells and Pro-angiogenic Activities: Roles in Tumor Progression', *Frontiers in immunology*, 10(April), p. 771. doi: 10.3389/fimmu.2019.00771.

Carayannopoulos, L. N. *et al.* (2002) 'Cutting edge: murine UL16-binding protein-like transcript 1: a newly described transcript encoding a high-affinity ligand for murine NKG2D.', *Journal of immunology (Baltimore, Md.: 1950)*, 169(8), pp. 4079–4083. doi: 10.4049/jimmunol.169.8.4079.

Celeste C., G. *et al.* (2016) 'Hepatitis C Virus–Induced Myeloid-Derived Suppressor Cells Suppress NK Cell IFN-γ Production by Altering Cellular Metabolism via Arginase-1', pp. 2283–2292. doi: https://doi.org/10.4049/jimmunol.1501881.

Cerwenka, A. *et al.* (2000) 'Retinoic acid early inducible genes define a ligand family for the activating NKG2D receptor in mice.', *Immunity*, 12(6), pp. 721–727. doi: 10.1016/s1074-7613(00)80222-8.

Chen, Y. *et al.* (2021) 'Reversible reprogramming of cardiomyocytes to a fetal state drives adult heart regeneration in mice', *Science*, 1540(September), pp. 1537–1540.

Chiche, A. *et al.* (2017) 'Injury-Induced Senescence Enables In Vivo Reprogramming in Skeletal Muscle', *Cell Stem Cell*, 20(3), pp. 407-414.e4. doi: 10.1016/j.stem.2016.11.020.

Chong, A. S. *et al.* (1994) 'CD54/ICAM-1 is a costimulator of NK cell-mediated cytotoxicity.', *Cellular immunology*, 157(1), pp. 92–105. doi: 10.1006/cimm.1994.1208.

Cikes, M., Friberg Jr., S. and Klein, G. (1973) 'Progressive Loss of H-2 Antigens With Concomitant Increase of Cell-Surface Antigen(s) Determined by Moloney Leukemia Virus in Cultured Murine Lymphomas23', *JNCI: Journal of the National Cancer Institute*, 50(2), pp. 347–362. doi: 10.1093/jnci/50.2.347.

Clevers, H. (2016) 'Modeling Development and Disease with Organoids', *Cell*, 165(7), pp. 1586–1597. doi: 10.1016/j.cell.2016.05.082.

Coudert, J. D. *et al.* (2005) 'Altered NKG2D function in NK cells induced by chronic exposure to NKG2D ligand-expressing tumor cells', *Blood*, 106(5), pp. 1711–1717. doi: 10.1182/blood-2005-03-0918.

Doeser, M. C., Schöler, H. R. and Wu, G. (2018) 'Reduction of Fibrosis and Scar Formation by Partial Reprogramming In Vivo', *Stem Cells*, 36(8), pp. 1216–1225. doi: 10.1002/stem.2842.

Dressel, R. *et al.* (2008) 'The tumorigenicity of mouse embryonic stem cells and in vitro differentiated neuronal cells is controlled by the recipients' immune response', *PLoS ONE*, 3(7). doi: 10.1371/journal.pone.0002622.

Dressel, R. *et al.* (2009) 'Multipotent adult germ-line stem cells, like other pluripotent stem cells, can be killed by cytotoxic T lymphocytes despite low expression of major histocompatibility complex class I molecules', *Biology Direct*, 4, p. 31. doi: 10.1186/1745-6150-4-31.

Dressel, R. *et al.* (2010) 'Pluripotent stem cells are highly susceptible targets for syngeneic, allogeneic, and xenogeneic natural killer cells', *The FASEB Journal*, 24(7), pp. 2164–2177. doi: 10.1096/fj.09-134957.

Frenzel, L. P. *et al.* (2009) 'Role of Natural-Killer Group 2 Member D Ligands and Intercellular Adhesion Molecule 1 in Natural Killer Cell-Mediated Lysis of Murine Embryonic Stem Cells and Embryonic Stem Cell-Derived Cardiomyocytes', *Stem Cells*, 27(2), pp. 307–316. doi: 10.1634/stemcells.2008-0528.

Guo, L. *et al.* (2019) 'Resolving Cell Fate Decisions during Somatic Cell Reprogramming by Single-Cell RNA-Seq', *Molecular Cell*, 73(4), pp. 815-829.e7. doi: 10.1016/j.molcel.2019.01.042.

Hafemeister, C. and Satija, R. (2019) 'Normalization and variance stabilization of single-cell RNA-seq data using regularized negative binomial regression', *Genome Biology*, 20(1), pp. 1–15. doi: 10.1186/s13059-019-1874-1.

Haridhasapavalan, K. K. *et al.* (2020) 'An Insight into Reprogramming Barriers to iPSC Generation', *Stem Cell Reviews and Reports*, 16(1), pp. 56–81. doi: 10.1007/s12015-019-09931-1.

Hoechst, B. *et al.* (2009) 'Myeloid derived suppressor cells inhibit natural killer cells in patients with hepatocellular carcinoma via the NKp30 receptor', *Hepatology*, 50(3), pp. 799–807. doi: 10.1002/hep.23054.

Huch, M. *et al.* (2013) 'Unlimited in vitro expansion of adult bi-potent pancreas progenitors through the Lgr5/R-spondin axis', *EMBO Journal*, 32(20), pp. 2708–2721. doi: 10.1038/emboj.2013.204.

Koch, C. A., Jordan, C. E. and Platt, J. L. (2006) 'Complement-Dependent Control of Teratoma Formation by Embryonic Stem Cells', *The Journal of Immunology*, 177(7), pp. 4803–4809. doi: 10.4049/jimmunol.177.7.4803.

de Lázaro, I. *et al.* (2019) 'Non-viral, Tumor-free Induction of Transient Cell Reprogramming in Mouse Skeletal Muscle to Enhance Tissue Regeneration', *Molecular Therapy*, 27(1), pp. 59–75. doi: 10.1016/j.ymthe.2018.10.014.

Li, P. *et al.* (2020) 'Dual roles of neutrophils in metastatic colonization are governed by the host NK cell status', *Nature Communications*, 11(1), pp. 1–14. doi: 10.1038/s41467-020-18125-0.

Liu, X. *et al.* (2020) 'Reprogramming roadmap reveals route to human induced trophoblast stem cells', *Nature*, 586(7827), pp. 101–107. doi: 10.1038/s41586-020-2734-6.

Lu, Y. *et al.* (2020) 'Reprogramming to recover youthful epigenetic information and restore vision', *Nature*, 588(7836), pp. 124–129. doi: 10.1038/s41586-020-2975-4.

Mosteiro, L. *et al.* (2016) 'Tissue damage and senescence provide critical signals for cellular reprogramming in vivo', *Science*, 354(6315). doi: 10.1126/science.aaf4445.

Ocampo, A. *et al.* (2016) 'In Vivo Amelioration of Age-Associated Hallmarks by Partial Reprogramming', *Cell*, 167(7), pp. 1719-1733.e12. doi: 10.1016/j.cell.2016.11.052.

Ohnishi, K. *et al.* (2014) 'Premature termination of reprogramming in vivo leads to cancer development through altered epigenetic regulation', *Cell*, 156(4), pp. 663–677. doi: 10.1016/j.cell.2014.01.005.

Oppenheim, D. E. *et al.* (2005) 'Sustained localized expression of ligand for the activating NKG2D receptor impairs natural cytotoxicity in vivo and reduces tumor immunosurveillance', *Nature Immunology*, 6(9), pp. 928–937. doi: 10.1038/ni1239.

Schwarz, B. A. *et al.* (2018) 'Prospective Isolation of Poised iPSC Intermediates Reveals Principles of Cellular Reprogramming', *Cell Stem Cell*, 23(2), pp. 289-305.e5. doi: 10.1016/j.stem.2018.06.013.

Senís, E. *et al.* (2018) 'AAVvector-mediated in vivo reprogramming into pluripotency', *Nature Communications*, 9(1), pp. 1–14. doi: 10.1038/s41467-018-05059-x.

Shibata, H. *et al.* (2018) 'In vivo reprogramming drives Kras-induced cancer development', *Nature Communications*, 9(1), pp. 1–7. doi: 10.1038/s41467-018-04449-5.

Siemaszko, J., Marzec-przyszlak, A. and Bogunia-kubik, K. (2021) 'Nkg2d natural killer cell receptor—a short description and potential clinical applications', *Cells*, 10(6). doi: 10.3390/cells10061420.

Spiegel, A. *et al.* (2016) 'Neutrophils suppress intraluminal NK cell-mediated tumor cell clearance and enhance extravasation of disseminated carcinoma cells', *Cancer Discovery*, 6(6), pp. 630–649. doi: 10.1158/2159-8290.CD-15-1157.

Stanietsky, N. *et al.* (2013) 'Mouse TIGIT inhibits NK-cell cytotoxicity upon interaction with PVR.', *European journal of immunology*, 43(8), pp. 2138–2150. doi: 10.1002/eji.201243072.

Sun, C. *et al.* (2017) 'High NKG2A expression contributes to NK cell exhaustion and predicts a poor prognosis of patients with liver cancer', *OncoImmunology*, 6(1), pp. 1–12. doi: 10.1080/2162402X.2016.1264562.

Sun, R. *et al.* (2020) 'Tumor-associated neutrophils suppress antitumor immunity of NK cells through the PD-L1/PD-1 axis', *Translational Oncology*, 13(10), pp. 1–9. doi: 10.1016/j.tranon.2020.100825.

Takahashi, K. and Yamanaka, S. (2006) 'Induction of pluripotent stem cells from mouse embryonic and adult fibroblast cultures by defined factors', *Cell*, 126(4), pp. 663–676. doi: 10.1016/J.CELL.2006.07.024.

Tumino, N. *et al.* (2021) 'Interaction Between MDSC and NK Cells in Solid and Hematological Malignancies: Impact on HSCT', *Frontiers in Immunology*, 12, pp. 1–10. doi: 10.3389/fimmu.2021.638841.

Wiemann, K. *et al.* (2005) 'Systemic NKG2D Down-Regulation Impairs NK and CD8 T Cell Responses In Vivo', *The Journal of Immunology*, 175(2), pp. 720–729. doi: 10.4049/jimmunol.175.2.720.

Yao, Y. and Wang, C. (2020) 'Dedifferentiation: inspiration for devising engineering strategies for regenerative medicine.', *NPJ Regenerative medicine*, 5, p. 14. doi: 10.1038/s41536-020-00099-8.

Zalfa, C. and Paust, S. (2021) 'Natural Killer Cell Interactions With Myeloid Derived Suppressor Cells in the Tumor Microenvironment and Implications for Cancer Immunotherapy', *Frontiers in Immunology*, 12(May). doi: 10.3389/fimmu.2021.633205.

Zappia, L. and Oshlack, A. (2018) 'Clustering trees: a visualization for evaluating clusterings at multiple resolutions', *GigaScience*, 7(7), pp. 1–9. doi: 10.1093/gigascience/giy083.

Zincarelli, C. *et al.* (2008) 'Analysis of AAV serotypes 1-9 mediated gene expression and tropism in mice after systemic injection', *Molecular Therapy*, 16(6), pp. 1073–1080. doi: 10.1038/mt.2008.76.

Figures

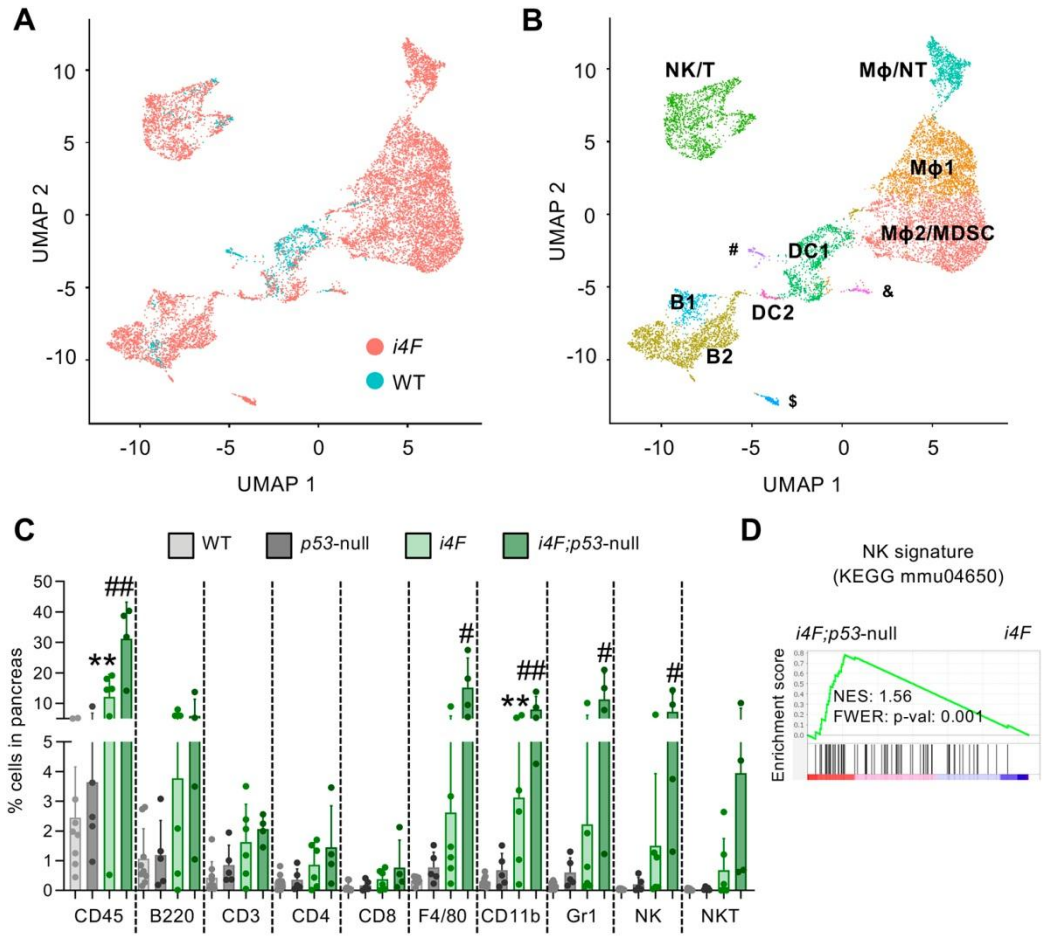

Figure 1 | Immune cell populations infiltrate the pancreas during *in vivo* reprogramming. A. UMAP plot visualizing immune cells infiltrated in the pancreas. WT (*n*=2) and *i4F* (*n*=3) mice were treated with doxycycline in the drinking water (1 mg/ml) for 1 week to induce partial reprogramming. **B**. UMAP plot of immune cell populations. Clusters were annotated using the most significant markers of each cluster and the FindAllMarkers function of Seurat (v3). The minor clusters correspond to endothelial cells (#), stellate cells (&) and marginal zone B cells ($). Mϕ = macrophages, NT = neutrophils, DC = dendritic cells, NK = natural killer cells, MDSC = myeloid derived suppressor cells, T = T cells and B = B cells. **C.** Flow cytometry analysis of main immune populations infiltrating in the pancreas after WT (*n*=9), *p53*-null (*n*=5), *i4F* (*n*=6) and *i4F*;*p53*-null (*n*=4) mice were treated with doxycycline for 7 days. Cell were gated from $DAPI^-/CD45^+$ cells. Data are pooled from 2 independent experiments. Graph represents mean ± SEM; statistical significance was evaluated using the

unpaired two-tailed Student's t test. ** P<0.01 (WT vs. *i4F*) and # P<0.05; ## P<0.01 (*i4F* vs. *i4F*;*p53*-null). **D.** Previously published RNA-sequencing data generated in our laboratory (Mosteiro *et al*., 2016) from the pancreas of *i4F* and *i4F*;*p53*-null (high reprogramming) mice was used to perform gene set enrichment analysis (GSEA) against a published signature (entry: mmu04650) of NK cell mediated cytotoxicity (KEGG).

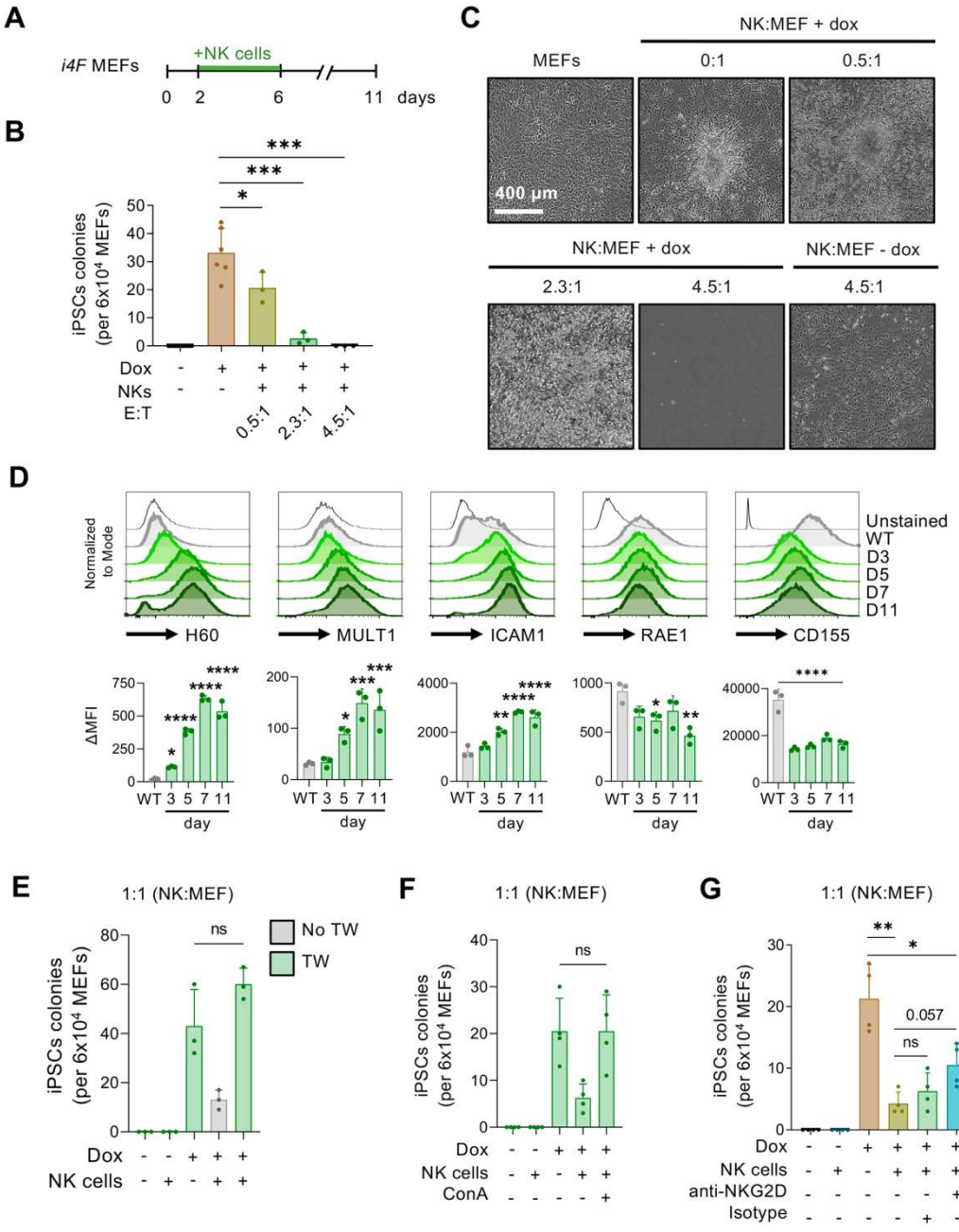

Figure 2 | NK cells eliminate partially reprogrammed cells *in vitro*. A. *i4F* MEFs were reprogrammed *in vitro* with doxycycline (1 µg/ml) for 11 days. From days 2 to 6, primed NK cells were added to the medium and cells were co-cultured for 5 days in co-culture medium**.** At day 11, iPSCs colonies were scored by Alkaline Phosphatase staining. **B**. Quantification and representative images (**C**) of NK cells co-cultured with *i4F* MEFs at effector:target (NK:MEF) ratios of 0.5:1, 2.3:1 and 4.5:1. Data pooled from 2 independent experiments. **D**. Representative flow cytometry plots and ΔMFI (Delta Mean Fluorescent Intensity) of the total H60, MULT1, ICAM1, RAE1 and CD155 expression in *i4F* MEFs reprogrammed with doxycycline (1 µg/ml) at different time

points (n=3). **E.** Co-culture experiment in which primed NK cells were seeded in transwells (TW) at NK:MEF ratio of 1:1 to avoid cell-to-cell contact (n=3). **F.** Co-culture experiment using concanamycin A (ConA) to disrupt the function of lytic granules secreted by NK cells. NK:MEF ratio of 1:1 (n=4). **G**. Co-culture experiment using the blocking antibody anti-NKG2D, which was added to the medium at days 2 and 4 of reprogramming (n=4). All graphs represent mean ± SD; *p<0.05, **p<0.001, ***p<0.001, ****p<0.0001 and statistical significance was evaluated using two-tailed Student's t-test (**B**, **E**, **F** and **G**) or one-way ANOVA (**D**).

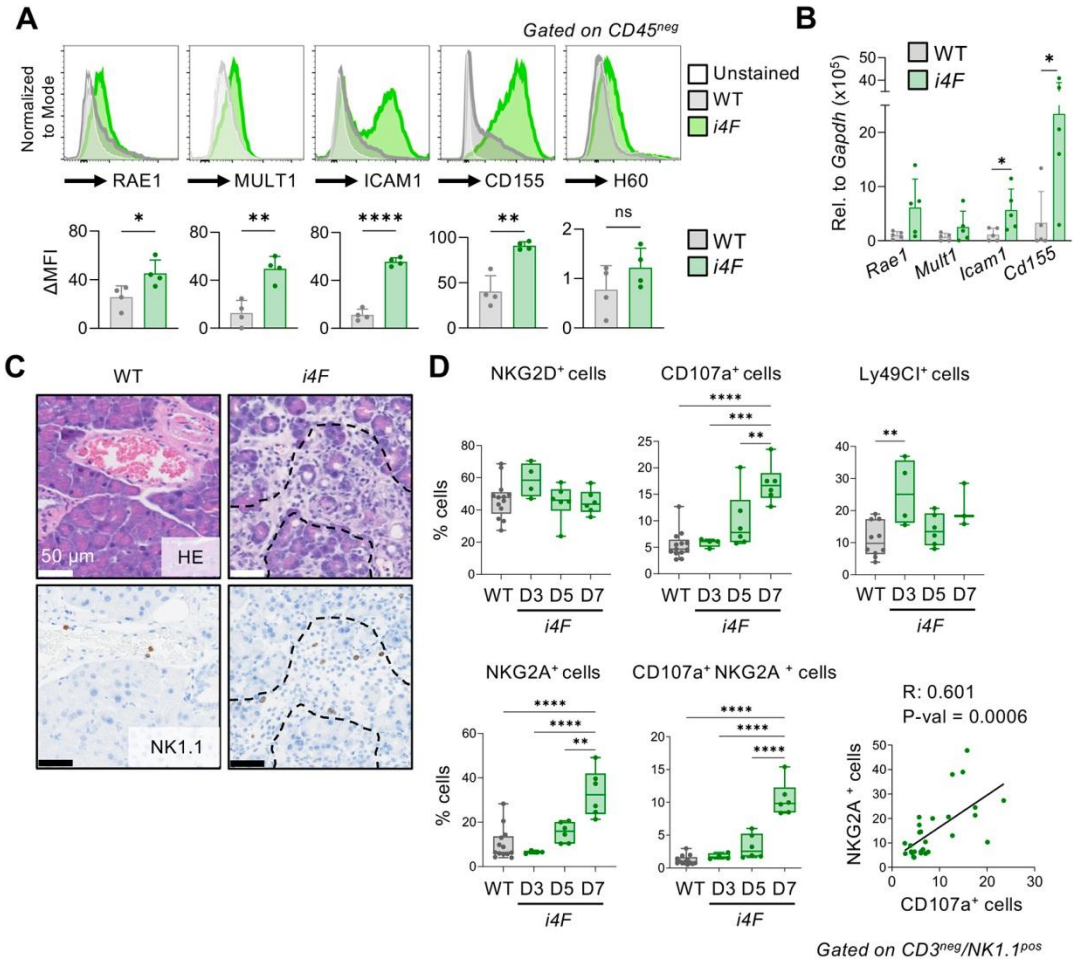

Figure 3 | NK cells recruited to the pancreas of *i4F* mice release lytic granules upon ligand-dependent activation. A. Representative flow cytometry plots and ΔMFI (Delta Mean Fluorescent Intensity) of the total RAE1, MULT1, ICAM1, CD155 and RAE1 expression in pancreas of WT and *i4F* mice treated with doxycycline (1 mg/ml) for 7 days. Graphs represent mean ± SD. **p*<0.05, ***p*<0.01, *****p*<0.0001, by two-tailed Student's t-test (*n*=4). **B.** WT and *i4F* mice were treated with doxycycline (1 mg/ml) for 7 days and expression levels of NK-activating ligands (*Rae1, Mult1, Icam1* and *CD155*) in pancreatic tissue were assessed by RT-qPCR. Graphs represent mean ± SD. **p*<0.05 by two-tailed Student's t-test (*n*=5). **C.** Representative images of NK1.1$^+$ cells in pancreas of WT and *i4F* mice treated with doxycycline for 7 days (*n*=5). **D.** Subpopulations of infiltrating NK cells in pancreas undergoing reprogramming at days 3 (D3), 5 (D5) and 7 (D7) of doxycycline treatment. Cell populations were gated on CD3$^-$ /NK1.1$^+$ cells and stained for the indicated activation, degranulation and inhibitory markers. Correlation of NKG2A$^+$ and CD107a$^+$ cells includes all time points. Graphs represent box with whiskers (min. to max); **p*<0.05, ***p*<0.01, ****p*<0.001, *****p*<0.0001 by one-way ANOVA (data pooled from 4 independent experiments).

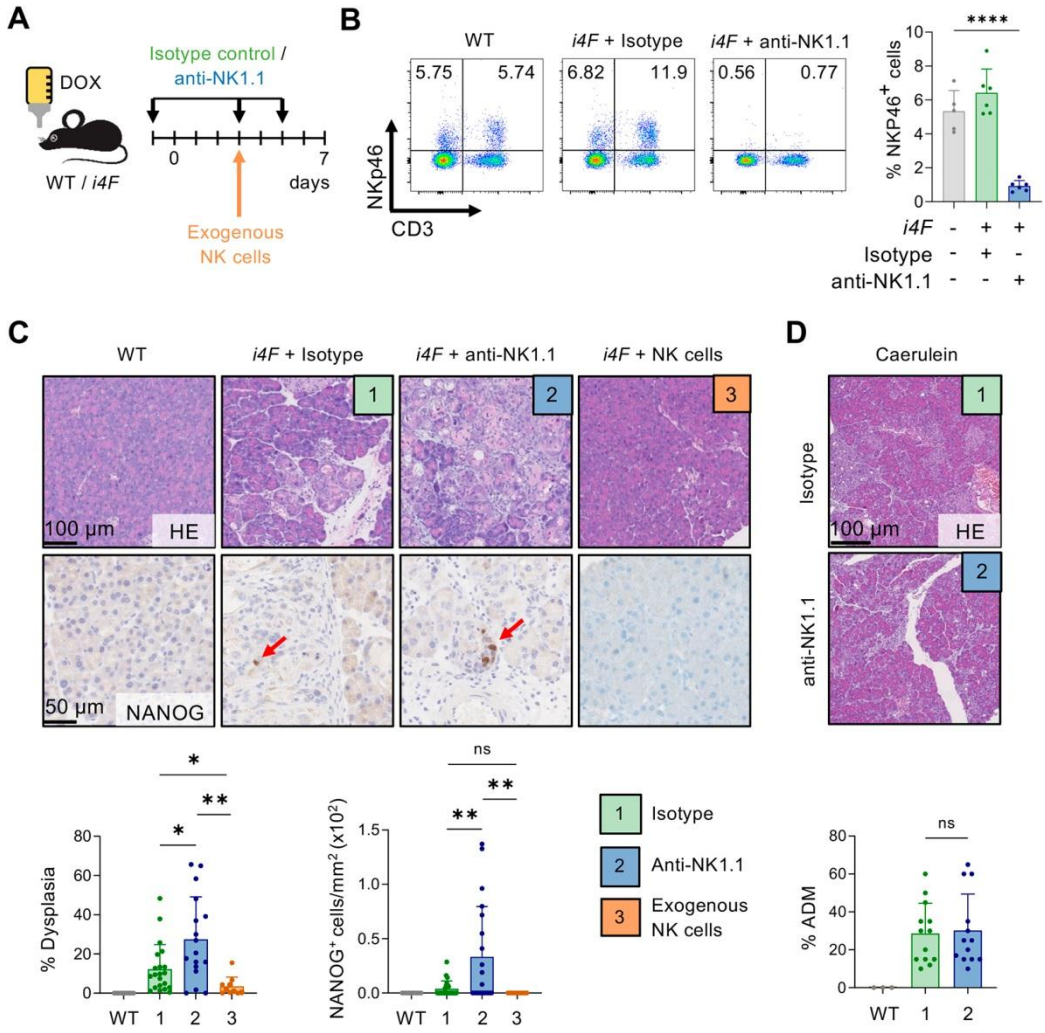

Figure 4 | NK cells are an extrinsic barrier for *in vivo* reprogramming. A. WT (*n*=10) and *i4F* mice were treated with doxycycline (1 mg/ml) for 7 days. *i4F* mice were treated with either isotype control antibody (1) (*n*=21) or anti-NK1.1 antibody (2) (*n*=17) (days -1, 3 and 5), or received adoptive transfer of 3.8 x 10^6 NK cells at day 3 of reprogramming (3) (*n*=10). **B**. Flow cytometry analysis of NK cells in blood of randomly selected mice at day 5 of reprogramming. NK cells gated as $CD3^-/NKp46^+$ cells (*n*=5 for WT+ dox and *n*=6 for *i4F* + isotype and *i4F* + anti-NK1.1 groups). **C.** Representative HE and NANOG staining (upper) and quantifications (lower). Data pooled from five independent experiments in conditions 1 and 2, and from 2 independent experiments in condition 3. **D.** Representative HE images of caerulein-induced pancreatitis (100 mg/kg, 7 times/day) for 2 days with isotype control or anti-NK1.1 treatment (*n*=13). Graphs represent mean ± SD; *p<0.05, **p<0.01, ****p<0.0001 and statistical significance was evaluated using two-tailed Student's t-test.

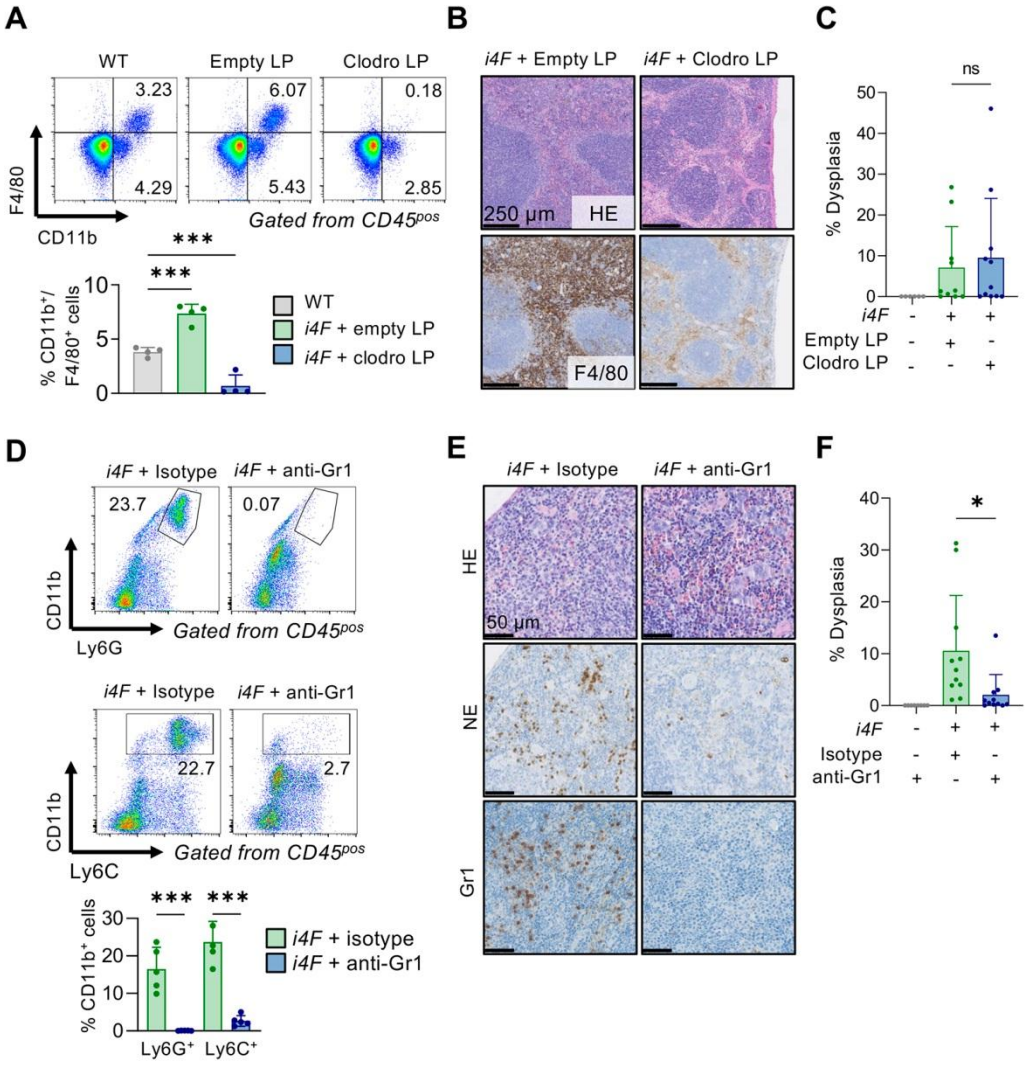

Figure 5 | Macrophage and Gr1$^+$ cell depletion during *in vivo* reprogramming. A. Representative flow cytometry plots and quantification of F4/80 and CD11b double positive populations in blood 16 hours after liposomes (LP) administration intraperitoneally at day 3 of reprogramming. Mice were randomly selected (*n*=4). Gated from CD45$^+$ cells. **B**. Representative HE and F4/80 immunohistochemistry of in the spleen of mice treated with doxycycline and empty or clodronate LP for 7 days. **C.** Dysplasia quantification in the pancreas of mice reprogrammed with empty or clodronate LP for 7 days (*n*=6 for WT, *n*=10 for empty LP and *n*=11 for clodronate LP groups). **D.** Representative flow cytometry plots and quantification of Ly6C and CD11b, and Ly6G and CD11b populations in blood at day 5 of reprogramming from mice treated with anti-Gr1 or isotype control antibodies. Gated from CD45$^+$ cells. **E**. Representative HE, neutrophil elastase (NE) and Gr1 immunohistochemistry in the spleen of partially reprogrammed mice treated with anti-Gr1 or isotype control antibodies for 7 days. **F**. Dysplasia quantification in the pancreas of mice

reprogrammed for 7 days with either anti-Gr1 or isotype control (n=8 for WT and n=11 for *i4F* and anti-Gr1 groups). Graphs represent mean ± SD; *p<0.05 and statistical significance was evaluated using two-tailed Student's t-test.

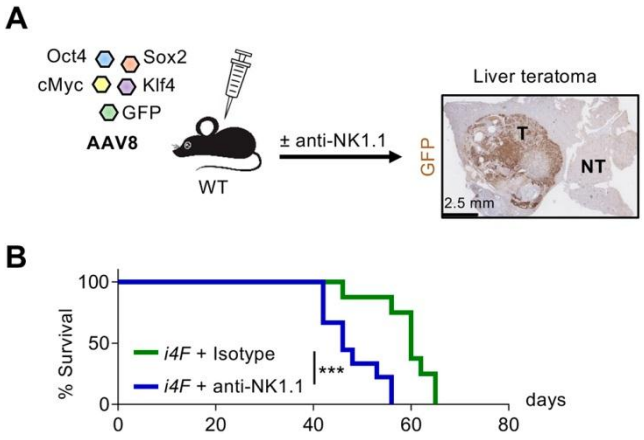

Figure 6 | NK1.1^{+} cell depletion enables full reprogramming and promotes teratoma formation. A. WT mice were retroorbitally injected with scAAV8 SFFV-hCO-O/K/S/M. A scAAV8 vector encoding GFP was additionally added as tracer. Anti-NK1.1 or isotype control antibodies were injected intraperitoneally at days -1, 3 and 5 during the first week, and then once a week until liver teratomas were palpable. T = teratoma; NT = non-teratoma. **B.** Survival curve upon teratoma formation in the liver. Data pooled from two independent experiments (n=9). Graph represents mean ± SD; ***p<0.001 and statistical significance was evaluated using log-rank (Mantel-Cox) test.

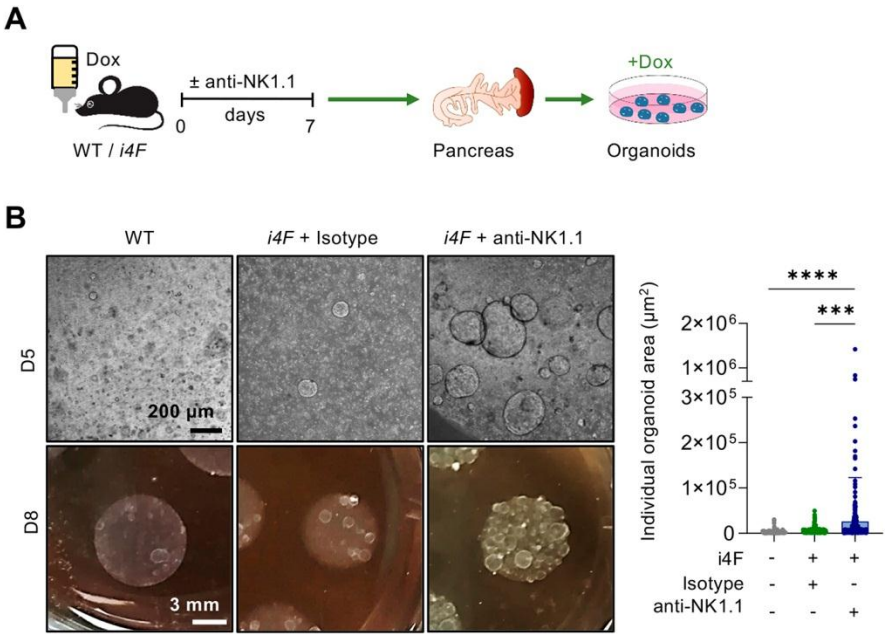

Figure 7 | NK1.1^{+} cell depletion promotes the survival of pancreatic cells with high plasticity. A. Mice were treated with doxycycline (dox) and anti-NK1.1 or isotype control antibodies for 7 days. Pancreata were dissociated to the single cell level and 3 x 10^5 cells/well were embedded in Matrigel per each condition (*n*=3) **B.** Representative images at day 5 (D5) and day 8 (D8) after seeding (left), and quantification of organoids size at D10 (right) (each dot represents one organoid from 3 biological replicates. A total 10 images were measured per sample)**.** Graph represents mean ± SD; ***p<0.001, ****p<0.0001 and statistical significance was evaluated using two-tailed Student's t-test.

Figure S1

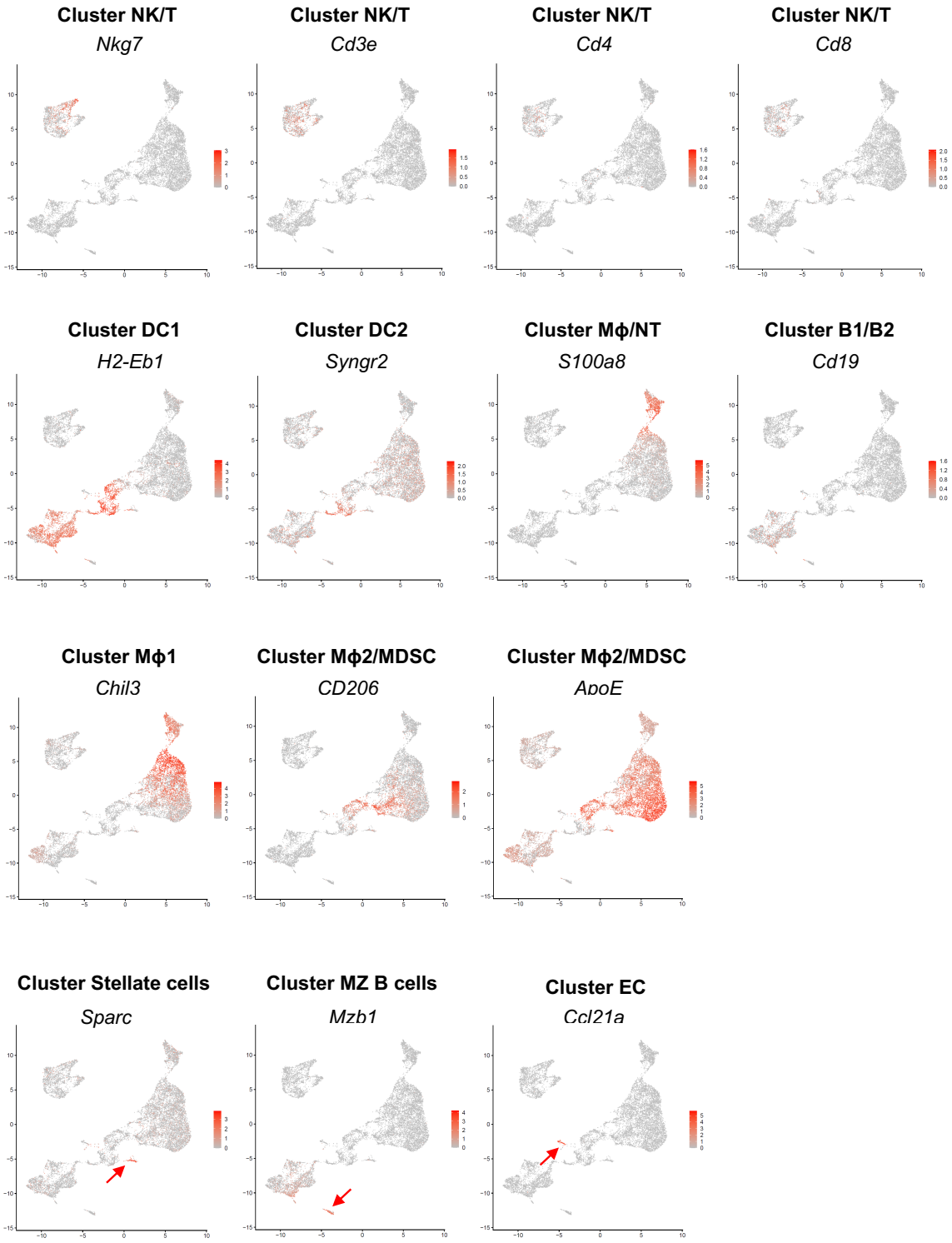

Fig. S1. UMAP showing the expression level of representative markers for each cell type. A. Top markers of each cluster are represented in UMAPs plots. Mϕ = macrophages, NT = neutrophils, DC = dendritic cells, NK = natural killer cells, T = T cells, B = B cells, EC = endothelial cells and MZ = marginal zone.

Figure S2

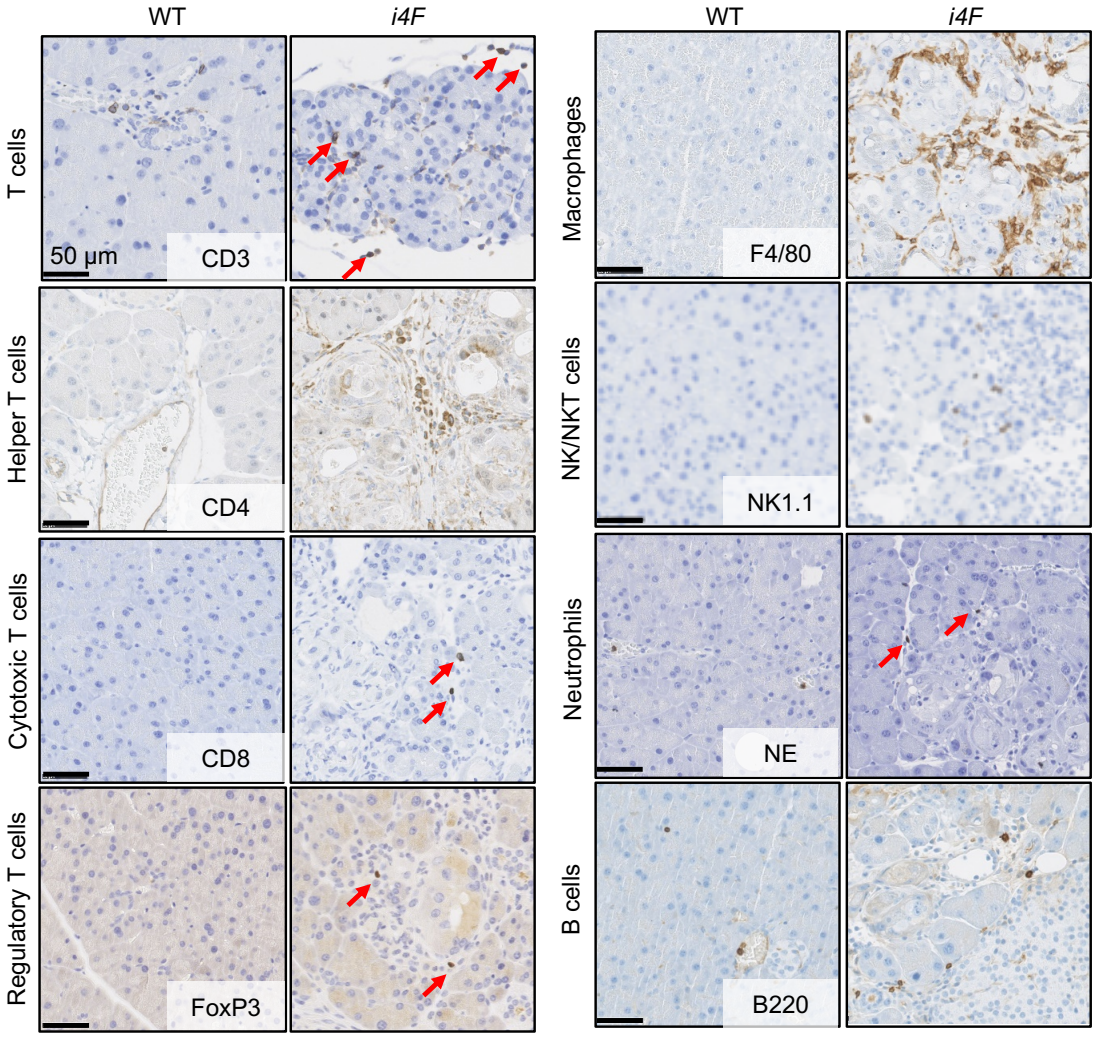

Fig. S2. Immune cells infiltrate partially reprogrammed pancreas. Representative images of partially reprogrammed pancreas at day 7 stained for the indicated immune cell markers (*n*=4): CD3 (T cells), CD4 (helper T cells), CD8 (cytotoxic T cells), FoxP3 (regulatory T cells), F4/80 (macrophages), NK1.1 (NK/NKT cells), NE (neutrophil elastase, neutrophils) and B220 (B cells).

Figure S3

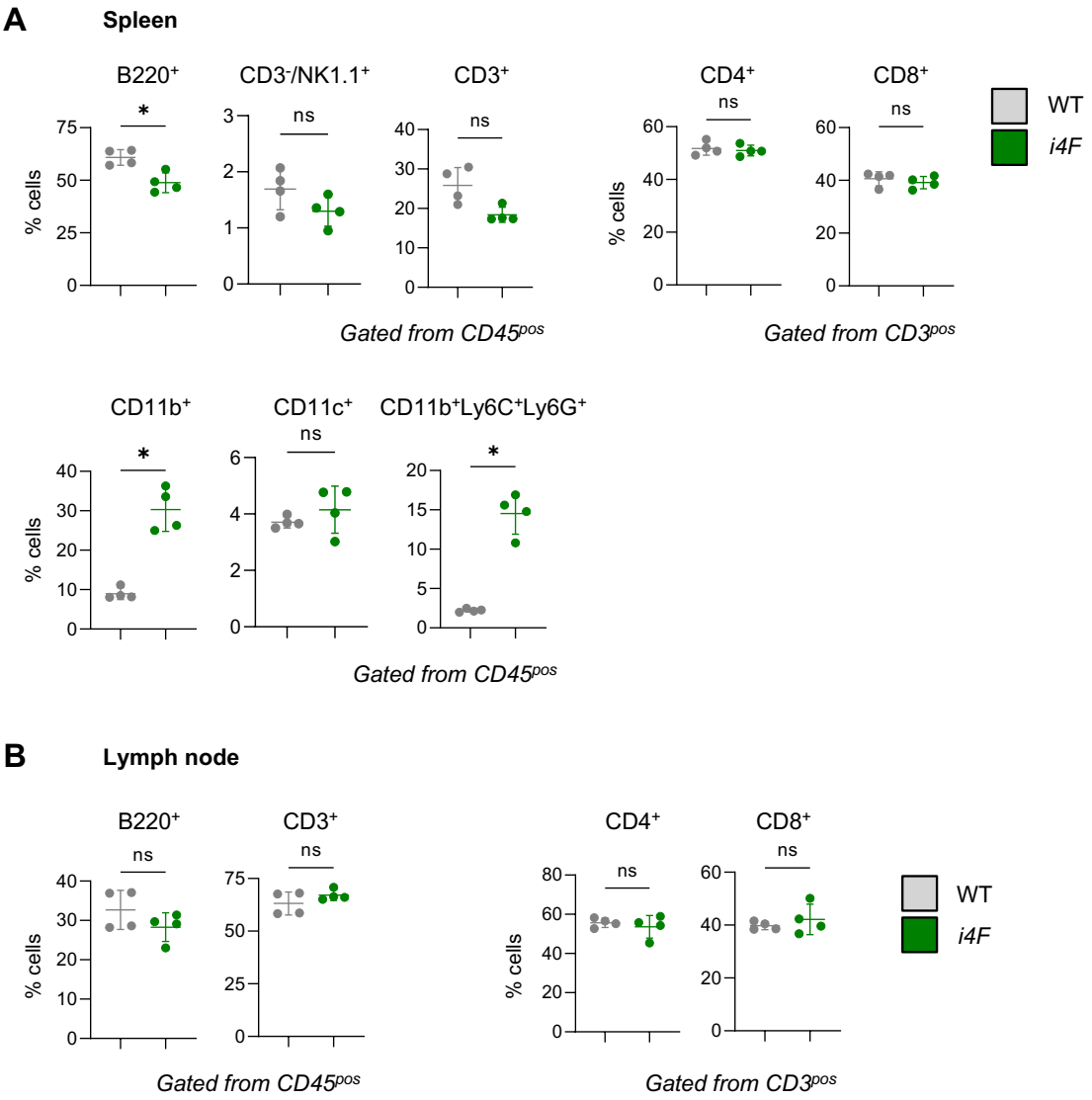

Fig. S3. Gr1$^+$ cells and CD11b$^+$ cells are upregulated in the spleen of *i4F* mice. Spleen and lymph nodes of *i4F* mice treated with doxycycline for 7 days (1 mg/ml) were harvested and most abundant immune populations were analysed by flow cytometry (*n*=4).

Figure S4

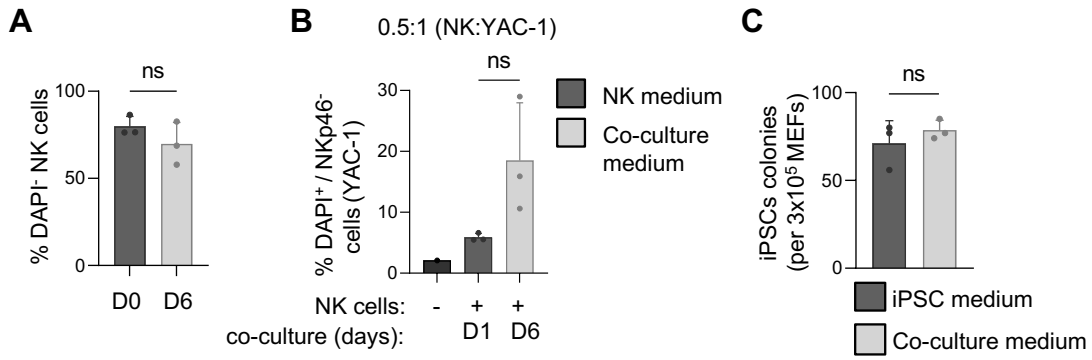

Fig. S4. Co-culture medium maintains NK cell survival and cytotoxicity, and iPSC colony formation. A. Viability of freshly isolated splenic WT NK cells and WT NK cells cultured in co-culture media for 6 days was analyzed. Gated from DAPI$^-$ cells (*n*=3). **B**. Splenic WT NK cells were either primed overnight in NK cell medium (D1) or maintained in co-culture medium for 5 more days (D6). Both conditions were co-cultured with YAC-1 cells for 4 hours to assess their cytotoxic capacity. Cell death was assessed using DAPI and NK cells were excluded using NKp46 antibody (*n*=3). **C**. *i4F* MEFs were reprogrammed *in vitro* with either iPSC medium for 11 days or with iPSC medium replaced by co-culture medium from days 2 to 6 of reprogramming. At day 11, iPSCs colonies were scored by Alkaline Phosphatase staining (*n*=3).

Figure S5

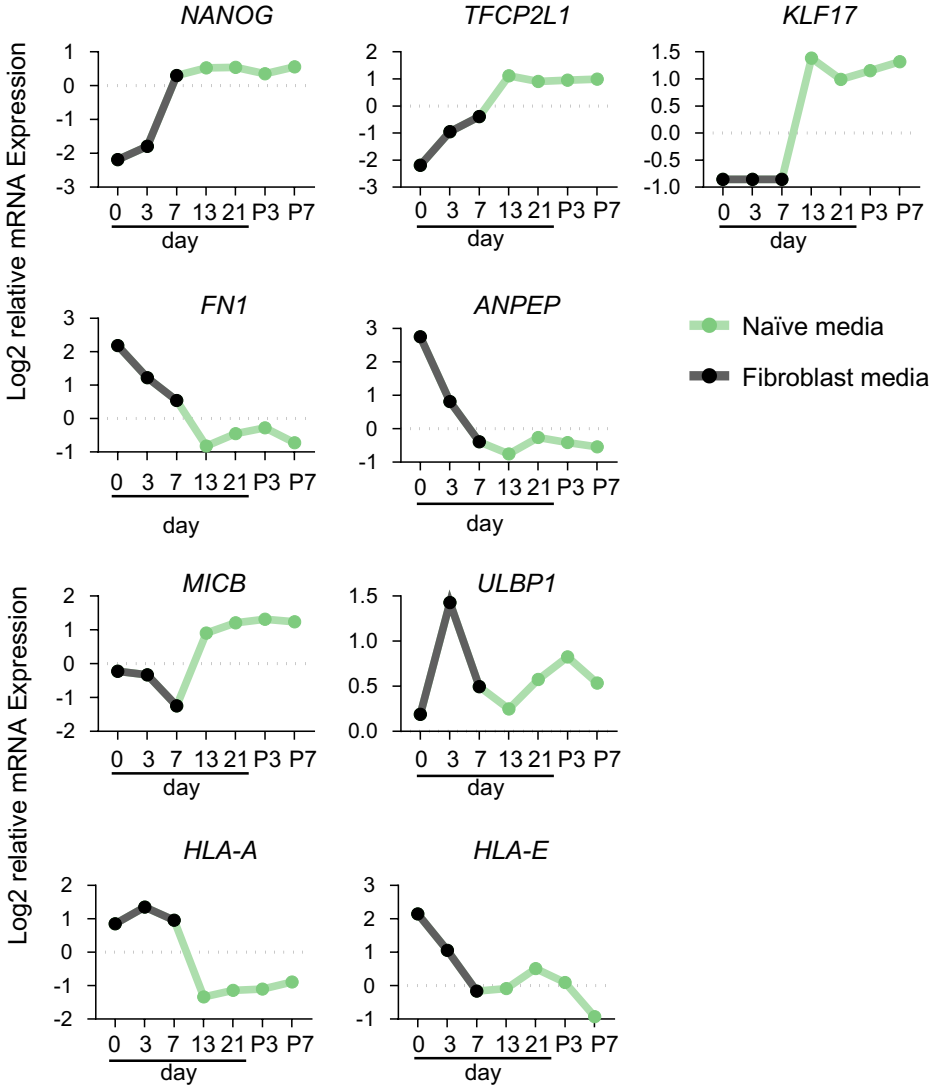

Fig. S5. Human fibroblasts upregulate NK-activating ligand MICB and downregulate MHC-I molecules during reprogramming. Previously published scRNAseq data from human dermal fibroblasts reprogrammed to naïve iPSCs for 21 days (Liu *et al.*, 2020). Cells were transduced with the transcription factors *OCT4*, *KLF4*, *SOX2* and *MYC*, and cultured in fibroblast medium for 7 days. Medium was changed to naïve medium at day 8 and cells were cultured until day 21. Relative mRNA expression of marker genes associated with pluripotency (*NANOG*, *TFCP2L1* and *KLF17*), human fibroblasts (*FN1* and *ANPEP*), NK-activating ligands (*MICB* and *ULBP1*) and MHC-I molecules (*HLA-A* and *HLA-E*) are represented at days 0, 3, 7, 13 and 21, and passages (P) 3 and 7.

Figure S6

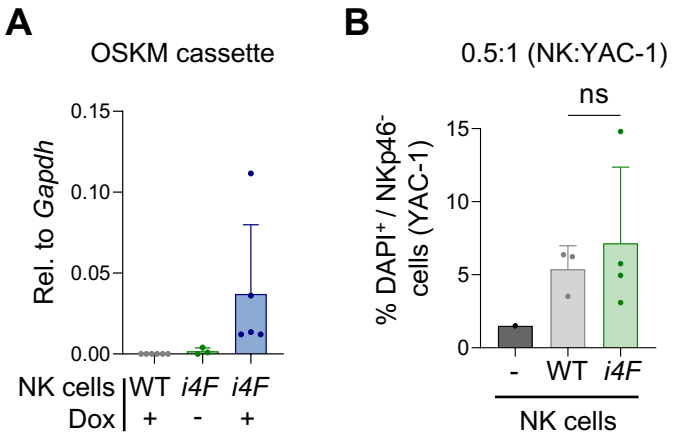

Fig. S6. NK cells maintain their cytotoxic activity upon OSKM induction. A. Spleens were harvested and NK cells were isolated on day 7 post-doxycycline (dox) initiation. Expression of the OSKM transgene was assessed by RT-qPCR (*n*=5 for WT+ dox and *i4F* + dox groups, and *n*=3 for *i4F* group). **B**. Percentage of DAPI^{+} YAC-1 cells lysed by WT or *i4F* NK cells. Mice were reprogrammed *in vivo* for 5 days and NK cells were isolated from the spleen. NK cells were primed *in vitro* with IL-2 and IL-15 in NK media for 6 days in the presence of doxycycline (1 µg/ml). A cytotoxic assay using YAC-1 as target cells was done after 4 hours of co-culture. Cell death was assessed using DAPI and NK cells were excluded using NKp46 antibody (*n*=3 for WT and *n*=4 for *i4F* group).

Figure S7

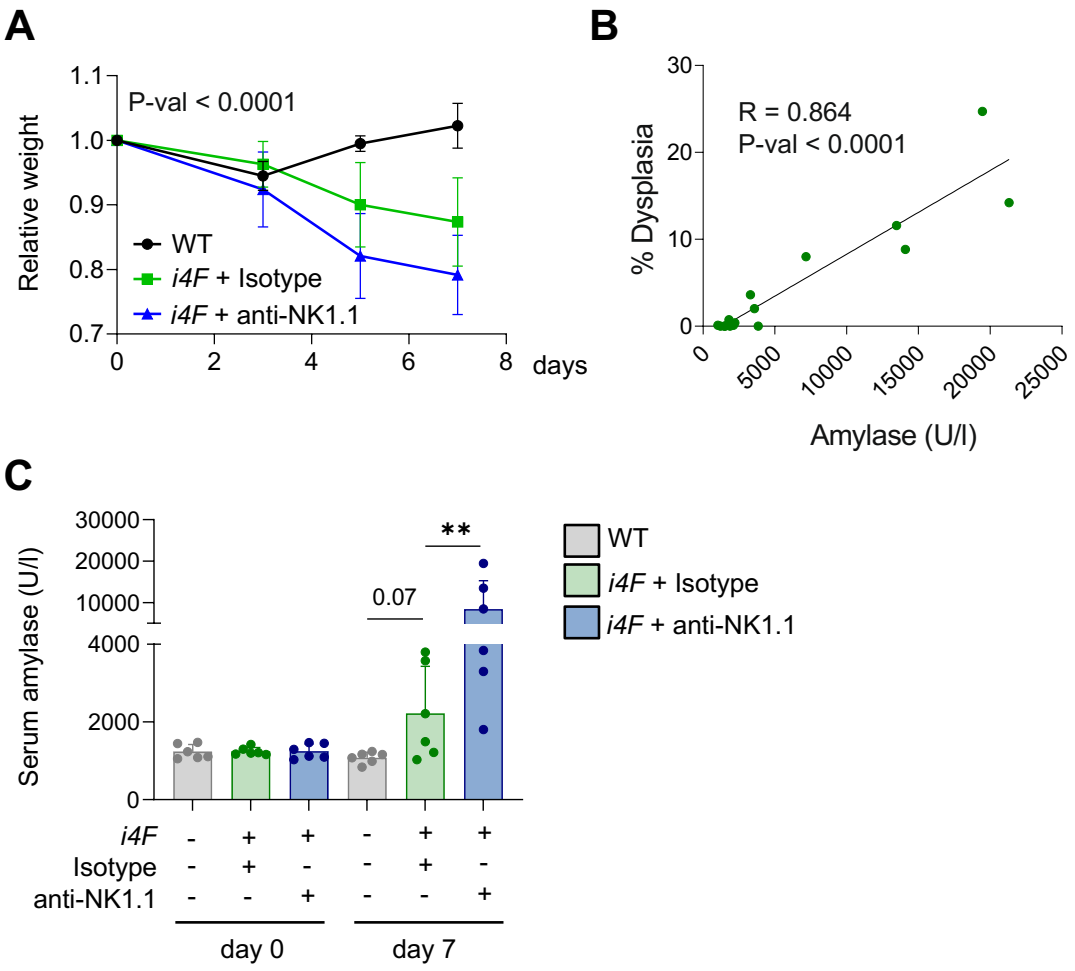

Fig. S7. Reprogrammed *i4F* mice treated with anti-NK1.1 lose more weight and have higher levels of amylase in serum than *i4F* mice treated with isotype control antibody. A. Relative weight loss of mice treated with doxycycline and anti-NK1.1 or isotype control antibodies for 7 days (n = 6). **B**. Correlation between amylase in serum and percentage of dysplasia in pancreas of *i4F* mice at day 7 of reprogramming (n=12). **C**. Amylase levels in serum at days 0 and 7 from reprogrammed mice treated with anti-NK1.1 or isotype control antibodies (n = 6). Graphs represent mean ± SD; **p<0.01 and statistical significance was evaluated using simple lineal regression (**A** and **B**) and two-tailed Student's t-test (**C**).

Table S1. List of primers used for mRNA expression analyses.

Name	Forward	Reverse
E2A-cMyc	GGCTGGAGATGTTGAGAGCAA	AAAGGAAATCCAGTGGCGC
Rae1	ACCCGAATGCAGACAGGAAGTTGA	GGACCTTGAGGTTGATCTTGGCTT
Mult1	CAATGTCTCTGTCCT CGGAA	CTGAACACGTCTCAGGCACT
Icam1	CTGTTTGAGCTGAGCGAGAT	AGGGTGAGGTCCTTGCCTAC
Cd155	CAACTGGTATGTTGGCCTCA	ATTGGTGACTTCGCACACAA
Gapdh	AGGTCGGTGTGAACGGATTTG	TGTAGACCATGTAGTTGAGGTCA

Table S2. List of fluorescent antibodies used for cytometry analyses.

Antibody	Source	Identifier	Dilution
B220 PE	Biolegend	103207	1:200
CD107a BV711	Biolegend	564348	1:100
CD11b A488	BioLegend	101219	1:200
CD11b BV786	BD Biosciences	740861	1:200
CD11b PECy7	eBioscience	25-0112-82	1:300
CD11b PerCPCy5.5	eBioscience	45-0112-82	1:400
CD11c PE-Vio 770	Milteny Biotec	130-110-840	1:200
CD155 PE-Cy7	Biolegend	131512	1:200
CD19-B220 APC-eF780	eBioscience	47-0452-80	1:200
CD3 AF700	eBioscience	56-0032-82	1:100
CD3 APC	eBiosciences	17-0032-80	1:300
CD3 FITC	Biolegend	100203	1:100
CD3ϵ PerCPCy5.5	Biolegend	100327	1:100
CD4 APC-eFluor780	eBioscience	47-0041-80	1:200
CD4 PE EF610	eBioscience	61-0042-80	1:400
CD45 BV605	Biolegend	103139	1:400
CD45 PE	BD Biosciences	553081	1:400
CD45 PerCP	BioLegend	103130	1:200
CD54/ICAM1 FITC	eBioscience	11-0541-82	1:200
CD8 BV786	BD Biosciences	563332	1:400
CD8 FITC	eBioscience	11-0081-82	1:400
F4/80 AF647	BioLegend	123122	1:100
F4/80 APC	BioLegend	123115	1:100
H60 APC	Milteny Biotec	130-108-821	1:100
Ly49CI BV421	BD Biosciences	744027	1:100
Ly6C FITC	BD Biosciences	561085	1:300
Ly6G PE	BD Biosciences	561104	1:300
NK1.1 APCCy7	BioLegend	108723	1:400
NK1.1 BV711	Biolegend	108745	1:200
NKG2A/CD159A PECy7	Biolegend	142809	1:100
NKG2D/CD314 PE	Biolegend	130207	1:100
NKp46-APC/Fire™ 750	BD Biosciences	137631	1:50
Rae1 Pan FITC	Milteny Biotec	130-111-468	1:50
ULBP1/MULT1 PE	R&D Systems	FAB2588P	1:100